Supplementary Material (ESI) for Physical Chemistry Chemical Physics
This journal is © The Royal Society of Chemistry 2013

Electronic Supplementary Information

Stabilizing effects of electrostatic *vs* aromatic interaction in diproline nucleated peptide β-hairpins

Kamlesh Madhusudan Makwana,[a] Srinivasarao Raghothama*[b] and Radhakrishnan Mahalakshmi*[a]

Contents:

Materials and Methods

Supplementary Figures and Tables

Materials and Methods:

a) Reagents and Chemicals:

All the solvents and reagents used for peptide synthesis including DMF, piperidine, DIPEA (N, N-diisopropylethylamine), Kaiser test kit and the cleavage reaction like TFA, phenol, thioanisole, ethanedithiol were purchased from Sigma-Aldrich Co. LLC. Rink amide AM resin (0.63meq, 200-400 mesh) was purchased from Novabiochem (EMD Millipore Chemicals). Fmoc protected amino acids and HATU (2-(1H-7-Azabenzotriazol-1-yl)--1,1,3,3-tetramethyl uranium hexafluorophosphate methanaminium) were purchased from GL Biochem Shanghai Ltd. Side chain protecting groups were chosen as follows: Mtr for ariginine, *t*Bu for tyrosine, Trt or *t*Bu for cysteine, Trt for histidine and Boc for lysine. Unless stated otherwise, all chemicals commercially obtained were >99% pure and used without further processing or purification.

b) Peptide Design:

The strategy employed in peptide design (Figure S1) and choice of amino acids is as follows:

1. The peptide length was fixed at 12 residues. This would allow for atleast two pairs of hydrogen bonds and a third pair if the termini are not frayed. This would also provide two diagnostic $d_{\alpha\alpha}$ NOEs between the $C^{\alpha}H$ of residues at the non-hydrogen bonding position. Both NOEs would serve as indicators of extent of strand registry.
2. ^{D}Pro-^{L}Pro segment was employed for turn nucleation.[1]
3. Valine was chosen at position 5, preceding ^{D}Pro. Of the 20 naturally occurring amino acids, Xxx-Pro bonds have the largest propensity of adopting the *cis* conformation.[2] As the *cis* conformation is undesirable in peptide hairpins, residues that minimize *cis-trans* isomerization need to be chosen at the position preceding ^{D}Pro6. It has been known that β-branched residues reduce conformational interconversion of the Xxx-Pro bond.[2g] Valine has previously been extensively employed at position '*i*' of turn segments in designed sequences and well-folded peptide hairpins have been obtained.[1, 3] Additionally, Val favors the extended conformation (being a β-branched amino acid).[4]
4. Leucine was positioned immediately after the turn, as this residue has also been extensively employed at position 'i+3' of turns in peptide hairpins.[1, 3a-c] Assignment of the spin system of this amino acid is also convenient in the NMR spectrum.
5. Positively charged residues such as Arg and Lys were included in the sequence to aid peptide solubilization in polar solvents. They were specifically positioned towards the N- and C-termini, respectively, to minimize peptide aggregation.[5] Additionally, the peptide was designed with a free N-terminus and a C-terminal amide unit arising from the resin after cleavage.

6. Phenylalanine residues were placed towards the termini, at positions 2 and 11. It was anticipated that in a well-folded hairpin the side chains of Phe residues will interact in a manner similar to that observed in peptide hairpins described earlier.[1, 6] Additionally, anomalous Phe ring proton chemical shifts would also be an indicator of the population of well-folded hairpins with registered strand segments.
7. This peptide was considered as an attractive system to investigate aromatic interactions *vs* electrostatic interactions between the side chains of Tyr, His and Cys residues. His was placed at position 9 (non-hydrogen bonding position). In peptide **C4H9** and **C4H9-p**, Cys was placed at position 4 in order to examine a Cys-His interaction. Similarly, Tyr4 in peptide **Y4H9** and **Y4H9-p** can be expected to interact with His9 at the non-hydrogen bonding position.
8. Threonine was chosen at position 10 of the strand segment to aid NMR resonance assignment and impart solubility to the peptide. Threonine also favors extended conformations,[2b, 4c] and it was assumed that this residue would contribute to local strand stabilization.

c) Peptide Synthesis:

The list of peptides studied is provided in Table 1 as well as Table S1. All the peptides were synthesized by standard solid phase Fmoc chemistry using the Rink amide AM resin. Activation of the carboxyl group was achieved using HATU + DIPEA in dry DMF; alternately, activated OPfp esters were used directly in some cases. Both methodologies yielded comparable peptide quality with negligible side reactions. Each amino acid coupling reaction was carried out in dry DMF at least twice to ensure near-complete reaction at all available and free sites. Completion of each coupling reaction was monitored using Kaiser test, by drawing out a few resin particles after each reaction. After complete synthesis, peptides were Fmoc deprotected (using 20% piperidine in dry DMF) and cleaved off from the resin using the cleavage cocktail (100µl per milligram of resin) comprising TFA/water/phenol/thioanisole/ethanedithiol in ratios 82.5:5:5:5:2.5, respectively. This cleavage reaction was constantly monitored using mass spectrometry for its completion. The resin was filtered off, TFA removed by evaporation under vacuum, and the peptide was precipitated using cold ether. The precipitate was repeatedly washed with cold ether to remove residual cleavage cocktail reagents. Peptide precipitate thus produced was air-dried to remove the ether, and subjected to gel filtration to remove residual side-products and small molecule impurities of the cleavage reaction.

d) Peptide Purification and Mass Spectrometric Analysis:

All peptides were subjected to gel filtration on a manually packed (7ml, Sephadex G10 resin; Sigma-Aldrich Co. LLC) column and eluted using water pH 2.0 (acidified using TFA). Briefly, peptide

powder was dissolved in minimal volume of the gel filtration buffer (water, pH 2.0), and centrifuged at 15,000 x *g* to remove particulate material. The supernatant was directly applied to the column and eluted by gravitational flow. Fractions were monitored using absorbance of blank corrected elutions, at 272nm (Figure S2), corresponding to the absorbance of Tyr and Phe residues. Fractions containing the desired peptide were pooled and lyophilized to obtain a white powder. Peptides were checked for successful synthesis and presence of the desired mass on a micrOTOF-Q II spectrometer (Bruker Daltonik GmbH) for **C4H9** and **Y4H9** and on a Hewlett Packard LCMSD instrument for **C4H9-p** and **Y4H9-p**. Results of mass spectrometry analyses of all peptides are presented in Figure S3. Multiply charged states were observed for all peptides, due to the presence of protonated side chains of Arg and Lys residues, in addition to the free amino terminus, and are accordingly indicated in the spectra. Purity of all peptides was assessed by ^{1}H 1D NMR spectroscopy on a high field instrument (described below).

e) NMR Experiments:

2D ^{1}H NMR experiments (TOCSY and ROESY for **C4H9** and **Y4H9**) were carried out on a Bruker Avance III 500MHz (in deuterated methanol and water) as well as a Bruker Avance III 700MHz spectrometer equipped with a cryogenic probe (in deuterated methanol). 2D NMR experiments for **C4H9-p** and **Y4H9-p** in deuterated methanol were obtained on a Bruker DRX-500 spectrometer. Peptide concentrations in the order of 5-7mM were employed. Absence of aggregation at these concentrations was independently confirmed by serial dilution and examination of ^{1}H 1D line widths. One dimensional spectra were acquired using 32K data points and processed with 1.0Hz line broadening. Spectra were referenced to residual methyl resonance set at 3.316ppm,[7] or TMS. Referencing to water chemical shift was carried out for this medium. All 2D experiments were recorded in the phase sensitive mode using time proportional phase incrementation (TPPI) methods. TOCSY and ROESY experiments were performed by collecting 1024 data points in the f2 dimension and 256 or 512 data points in the f1 dimension. Experiment temperature used for each peptide was slightly adjusted to optimize both chemical shift dispersion (to facilitate complete resonance assignment) as well as NOE intensity and number. Variation in secondary structure content for all peptides was negligible over the temperature range examined, and this was independently established using CD experiments (data not shown). Solvent suppression was achieved using standard presaturation pulse program available in the Bruker library. NMR data were processed using Bruker Topspin v3.0 software for Windows. Data were zero filled to 2K points in the f1 dimension and a $\pi/2$ shifted sine squared window function was applied to the both dimensions prior to Fourier transformation.

f) ΔG Calculations:

$C^{\alpha}H$ chemical shifts of all residues except that of Tyr, Cys and $^{D/L}$Pro were used to estimate the free energy of folding for all peptides. Tyr and Cys were avoided so as to not introduce positional bias (hydrogen bonded *vs* non-hydrogen bonded) of $C^{\alpha}H$ shifts of these residues in the calculations.[8] The diproline segment, which resides in the turn region, was also excluded. The free N-terminus of the peptide could also not be considered due to rapid exchange with the solvent. Hence, the free energy values calculated essentially correspond to the contribution of the hairpin arms in maintaining strand registry. Random coil and beta-sheet chemical shifts were obtained from Biological Magnetic Resonance Bank (BMRB; http://www.bmrb.wisc.edu/;),[9] and were considered to represent the unfolded and folded conformations, respectively. Folded fraction was calculated for each residue using the following equation:

$$f_F = \frac{C_O - C_U}{C_F - C_U}$$

Here f_F corresponds to the folded fraction for each residue, C_O is the observed chemical shift, C_U is the chemical shift of the same residue in unfolded structures and C_F is the chemical shift in the fully folded form. The folded fraction determined for each residue included in the calculation was averaged and used for the calculation of equilibrium constant K_{eq} using the equation:

$$K_{eq} = \frac{f_F}{f_U} = \frac{f_F}{1 - f_F}$$

Here f_U corresponds to the unfolded fraction. At equilibrium, the sum of the folded and unfolded fractions corresponds to 1.0. The free energy of folding ΔG_F was then obtained using the equation:

$$\Delta G_F = -RT\ ln K_{eq}$$

Here R corresponds to the ideal gas constant and equals 1.9858 cal $K^{-1}mol^{-1}$ and T is the experiment temperature, in kelvin. Results are summarised in Table S2.

g) Electronic CD Experiments:

Far-UV CD spectra were recorded on Jasco J-815 or J-715 CD spectropolarimeter in methanol, water and methanol-water mixtures. Spectra were recorded using a 1mm cuvette between 195nm and 300nm at 0.5nm interval with a scan speed of 50nm/min, and averaged over 5 scans. Spectra were blank subtracted and smoothened. Titration experiments were carried out in steps of 5% with constant peptide concentration (water *vs.* methanol). Data were analysed using Spectra Manager v2.0 (Jasco Inc.) and plots were generated using SigmaPlot v11.0. For the titration experiments, values obtained at selected wavelengths (~200nm, ~216nm and ~223nm) for each peptide were normalized against their respective 100% methanol datasets and plotted against the corresponding methanol/water concentration.

h) Iodoacetamide Treatment:

Iodoacetamide is a light-sensitive, sulfhydrly-reactive alkylating reagent used to block reduced cysteine residues, resulting in the covalent addition of a carbamidomethyl group (57.0Da). Iodoacetamide does not react with disulphide bonds, and this protocol also facilitated detection of possible disulphide bonds formed in the peptides **C4H9** and **Y4H9** during the course of various studies carried out with either peptide.

Steps followed during iodoacetamide treatment of the peptide are:

1. 50µl of 1mM peptide dissolved freshly in water was taken in a vial.
2. The vial was thoroughly wrapped with aluminium foil in order to protect the reaction from light.
3. 50µl of 500mM iodoacetamide (in excess) was added dropwise to the vial.
4. The sample was then incubated in dark for about 3-4hours with gentle vortexing every 30min.

After completion of the incubation step, the sample was directly loaded onto a column with manually packed G10 matrix and purified as described earlier in **d)**. All elutions were subjected to mass spectrometric analysis. The mass spectra confirmed that the reaction was completed to >98%, indicating that non-specific dimerization through disulphide bonds was marginal in both peptides (Figure S3). The iodoacetamide treated forms of both parent peptides **C4H9** and **Y4H9** were labelled **C4H9-i** and **Y4H9-i**, respectively.

i) Structure Calculation:

Structure calculations for **C4H9** and **Y4H9** as well as their *t*Bu analogues were carried out using CYANA v2.1.[10] ^{D}Pro coordinates were added to the CYANA library; however *t*Bu was not included. Upper distance restrains were generated using NOE intensities that were assigned distance limits between 2.5Å and ~5.0Å by visual inspection. Additionally, 4 hydrogen bond constraints, obtained from variable temperature experiments, and 9 angle constraints obtained from the $^{3}J_{N\alpha}$ values, were applied during the refinement stage. Details of the constraints used for each peptide are provided in Table S3. A total of 100 structures were calculated for each peptide and rendered using PyMol.[11] Dihedral angles were calculated for the best 15 structures using PyMol and MolMol;[12] the data obtained are provided in Tables S4-S7. Note that error values in some dihedral angles are large since NOE constraints for these residues were very few or unavailable.

Supplementary Material (ESI) for Physical Chemistry Chemical Physics
This journal is © The Royal Society of Chemistry 2013

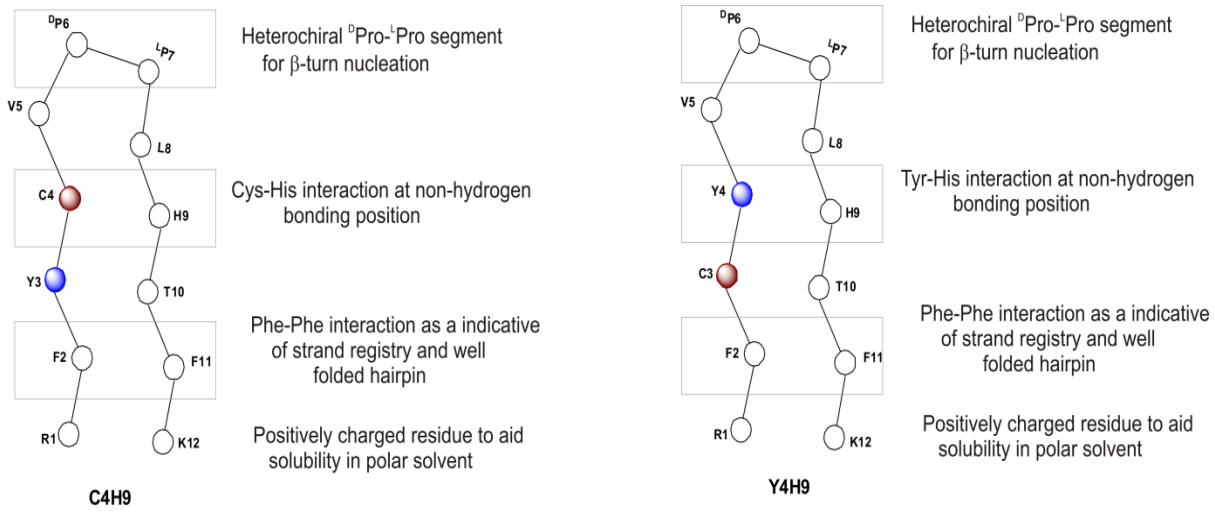

Figure S1: Summary of the salient features used in the design of peptides discussed in this study. The schematic is provided for the parent peptides **C4H9** and **Y4H9**. In the thiol-protected derivatives **C4H9-p** and **Y4H9-p**, the Cys residue has a *t*Bu protected side chain.

Table S1: List of peptide sequences discussed in this study along with their mass spectrometry analysis data (also see Table 1 of main text)

Peptide Name[a]	Sequence[b]	Mass spectral data (Da)			
		$M + H^+$	$[M + 2H^{2+}]/2$	$[M + 3H^{3+}]/3$	M_{calc}
C4H9	H_2N-RFYCV^{D}P^{L}PLHTFK-$CONH_2$	1506.79	753.90	502.94	1506.0
Y4H9	H_2N-RFCYV^{D}P^{L}PLHTFK-$CONH_2$	1506.78	753.89	502.93	1506.0
C4H9-p	H_2N-RFYC(*t*Bu)V^{D}P^{L}PLHTFK-$CONH_2$	1562.8	782.0	521.8	1562.0
Y4H9-p	H_2N-RFC(*t*Bu)YV^{D}P^{L}PLHTFK-$CONH_2$	1562.8	781.5	521.8	1562.0
C4H9-i	H_2N-RFYC(Cam)V^{D}P^{L}PLHTFK-$CONH_2$	1563.83	782.42	521.95	1563.0
Y4H9-i	H_2N-RFC(Cam)YV^{D}P^{L}PLHTFK-$CONH_2$	1563.83	782.41	521.94	1563.0

[a]C4H9-i and Y4H9-i were generated by treatment of the parent peptides with iodoacetamide.

[b]One letter code is used for the amino acids; *t*Bu = t-butyl group; Cam = carbamidomethyl group.

Supplementary Material (ESI) for Physical Chemistry Chemical Physics
This journal is © The Royal Society of Chemistry 2013

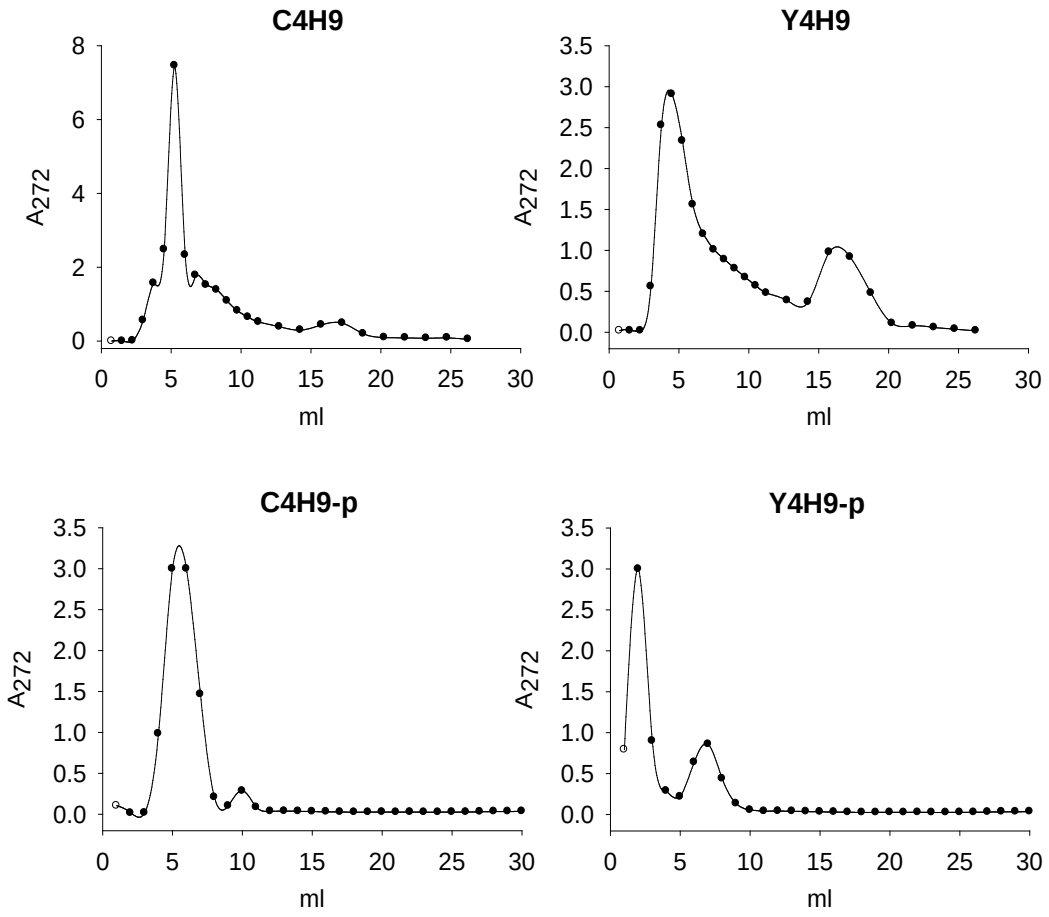

Figure S2: Representative gel filtration profiles of the peptides, monitored at 272nm. The largest peak in each profile corresponds to the desired peptide. Note that retention times may vary based on the packing efficiency of each column.

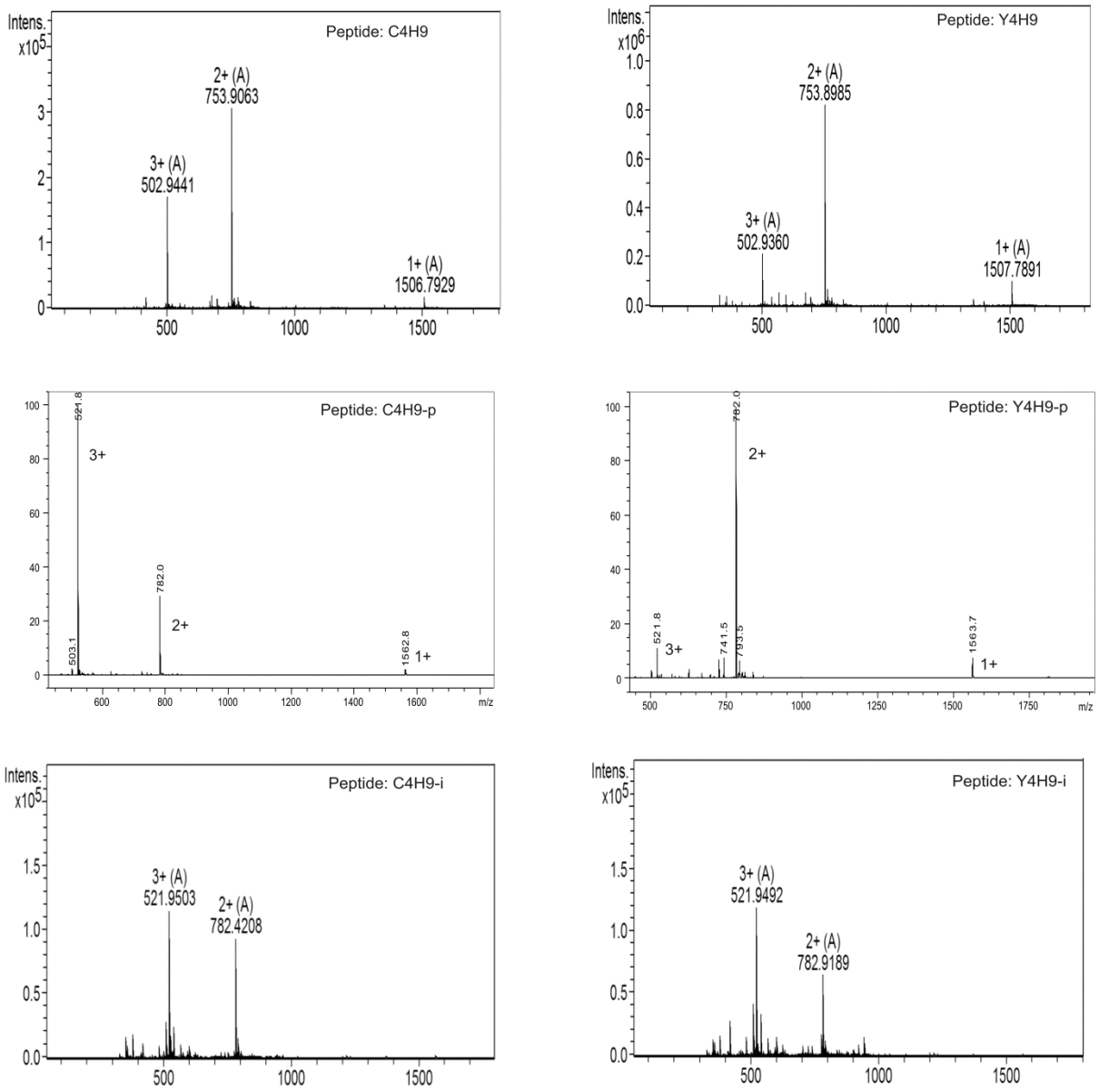

Figure S3: Mass spectrometric analysis of purified peptides. Mass spectral data for **C4H9**, **Y4H9, C4H9-i and Y4H9-i** (top and bottom panel) recorded on Bruker micrOTOF-Q II spectrometer and for **C4H9-p** and **Y4H9-p** (middle panel) recorded on a Hewlett Packard LCMSD instrument.

Supplementary Material (ESI) for Physical Chemistry Chemical Physics
This journal is © The Royal Society of Chemistry 2013

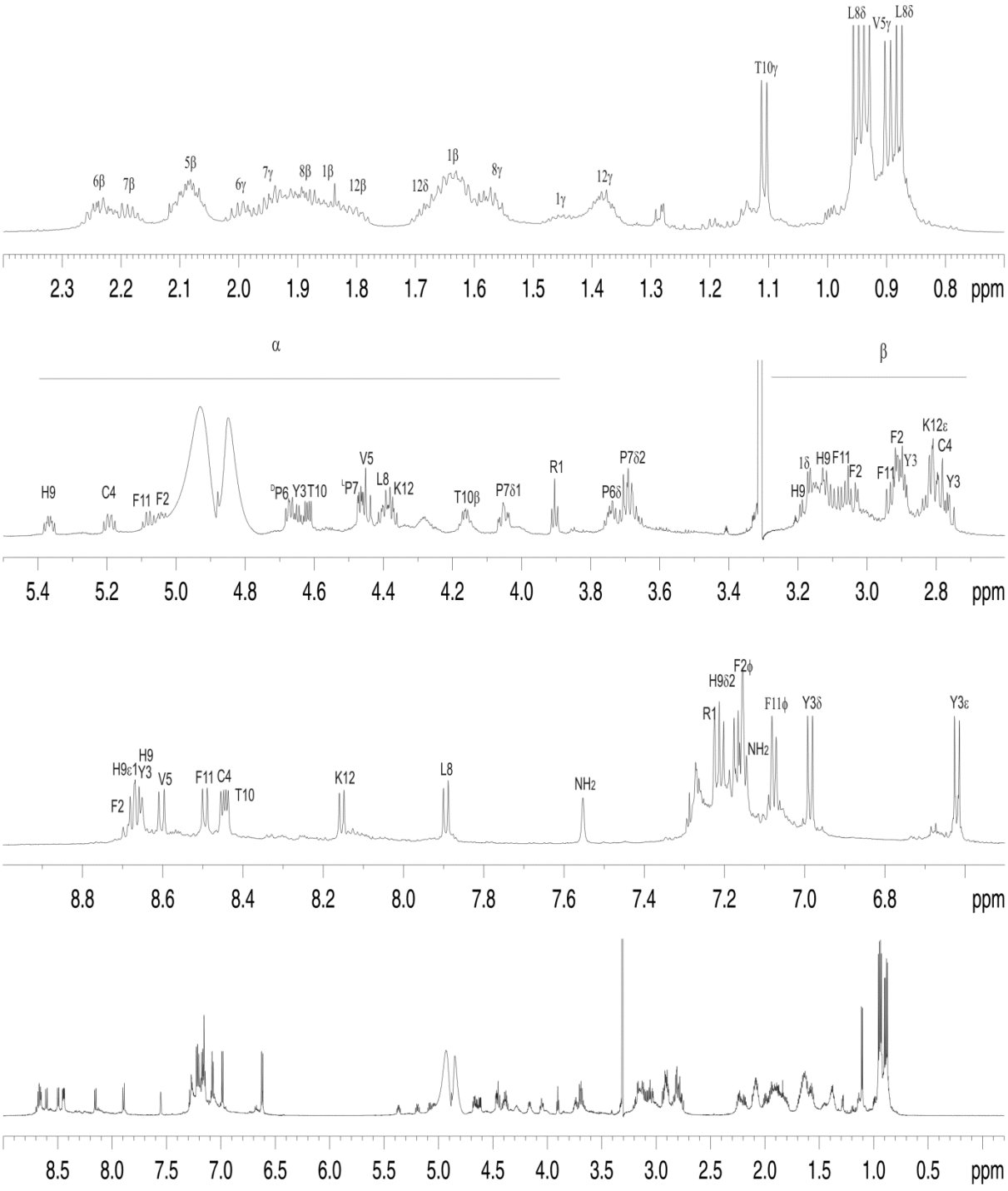

Figure S4 (a): 700MHz ^{1}H 1D spectrum of **C4H9** in CD_3OH at 298K. Complete assignment of the resonances was achieved using a combination of TOCSY and ROESY experiments.

Supplementary Material (ESI) for Physical Chemistry Chemical Physics
This journal is © The Royal Society of Chemistry 2013

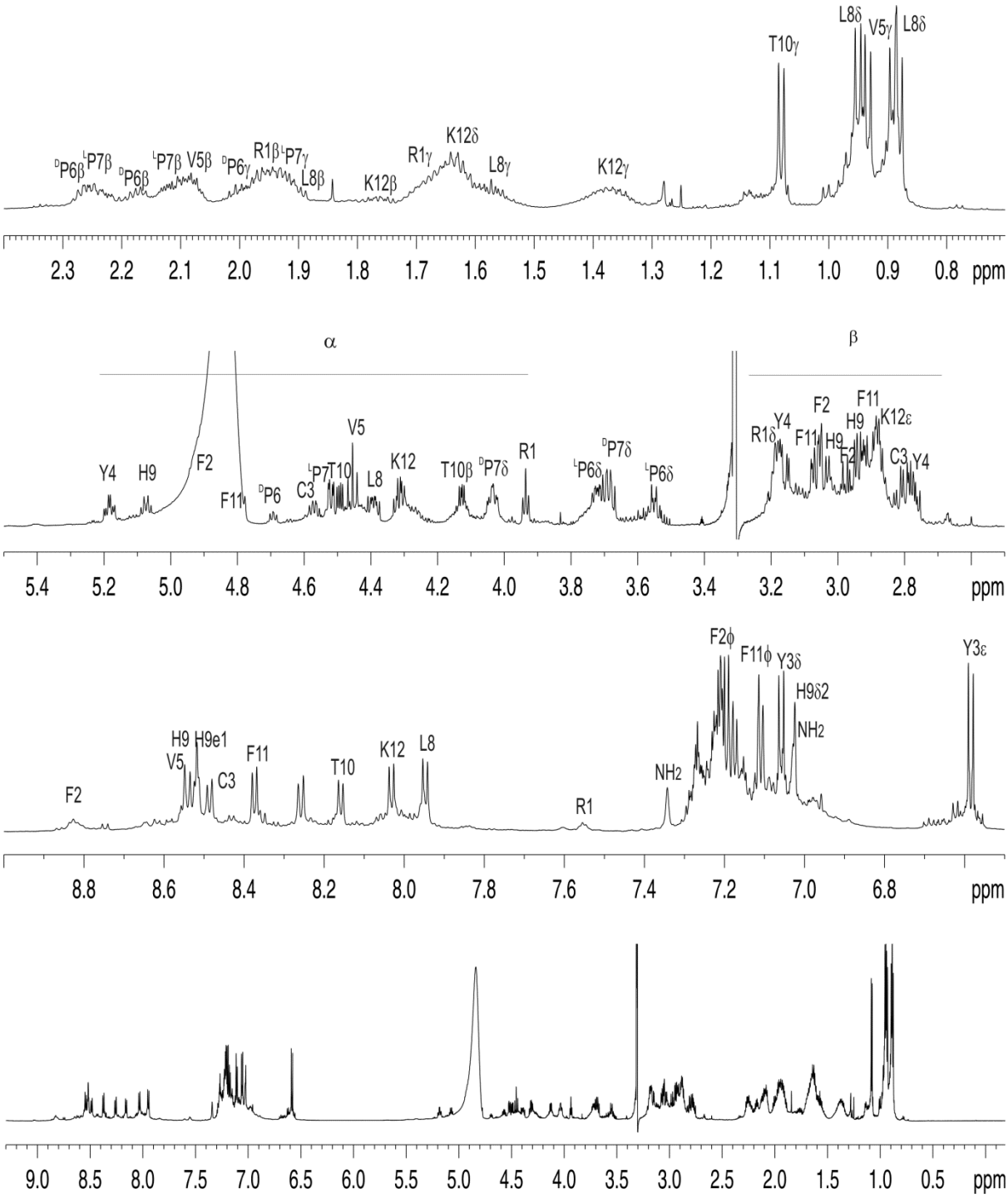

Figure S4 (b): 700MHz ^{1}H 1D spectrum of **Y4H9** in CD_3OH at 308K.Complete assignment of the resonances was achieved using a combination of TOCY and ROESY experiments.

Supplementary Material (ESI) for Physical Chemistry Chemical Physics
This journal is © The Royal Society of Chemistry 2013

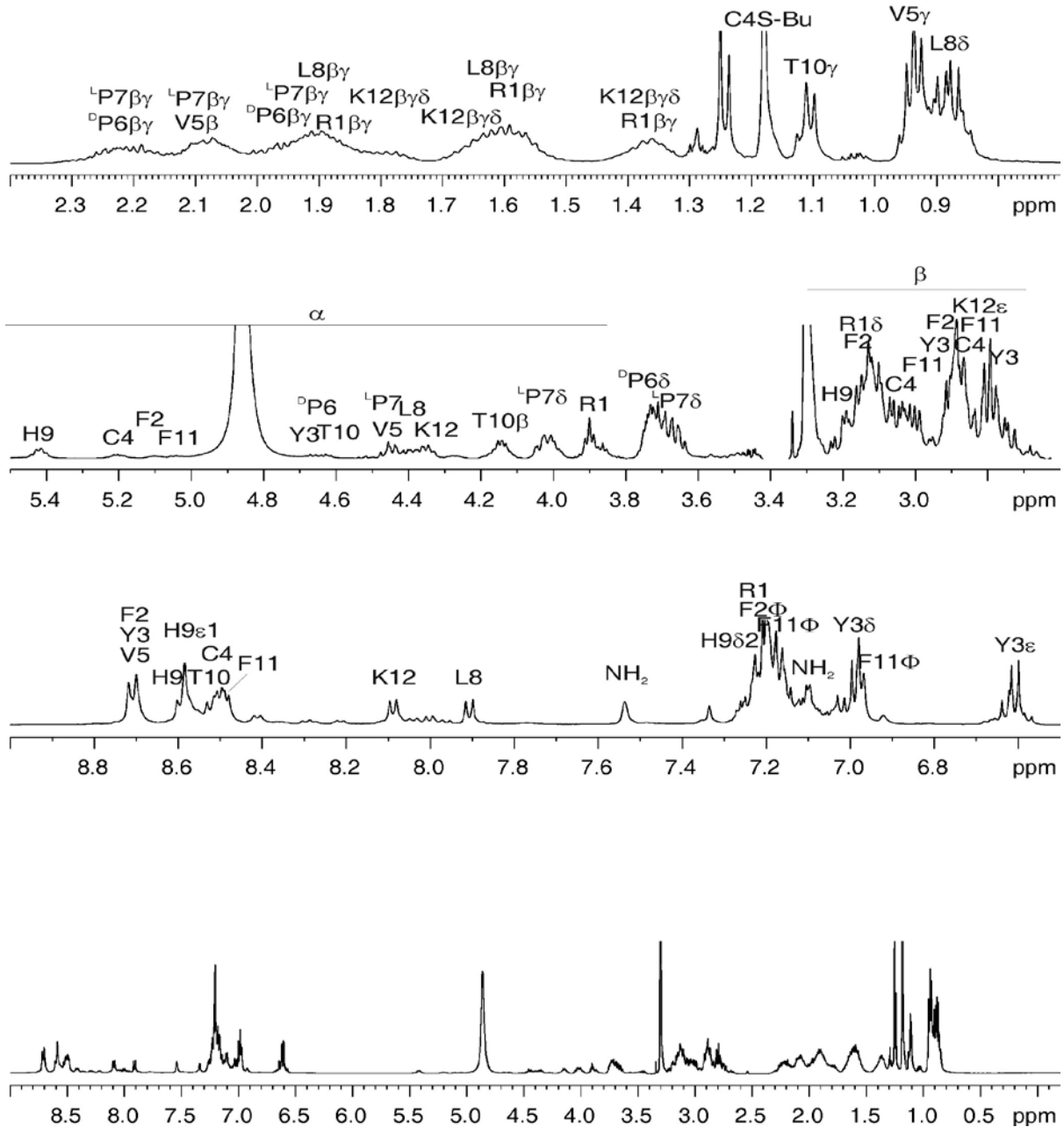

Figure S4 (c): 500MHz ^{1}H 1D spectrum of **C4H9-p** in CD_3OH at 303K.Complete assignment of the resonances was achieved using a combination of TOCSY and ROESY experiments.

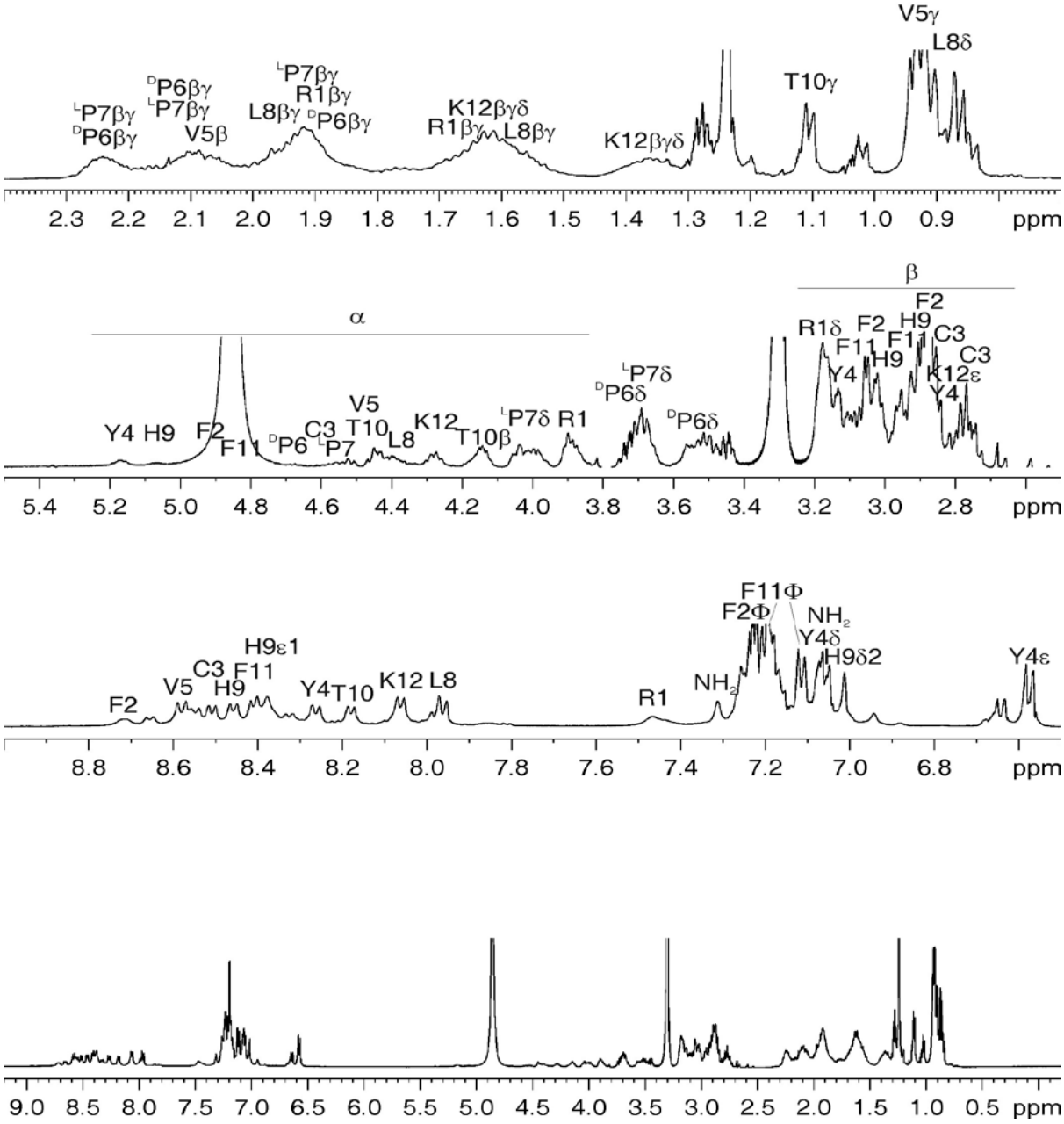

Figure S4 (d): 500MHz ^{1}H 1D spectrum of **Y4H9-p** in CD_3OH at 303K.Complete assignment of the resonances was achieved using a combination of TOCSY and ROESY experiments.

Supplementary Material (ESI) for Physical Chemistry Chemical Physics
This journal is © The Royal Society of Chemistry 2013

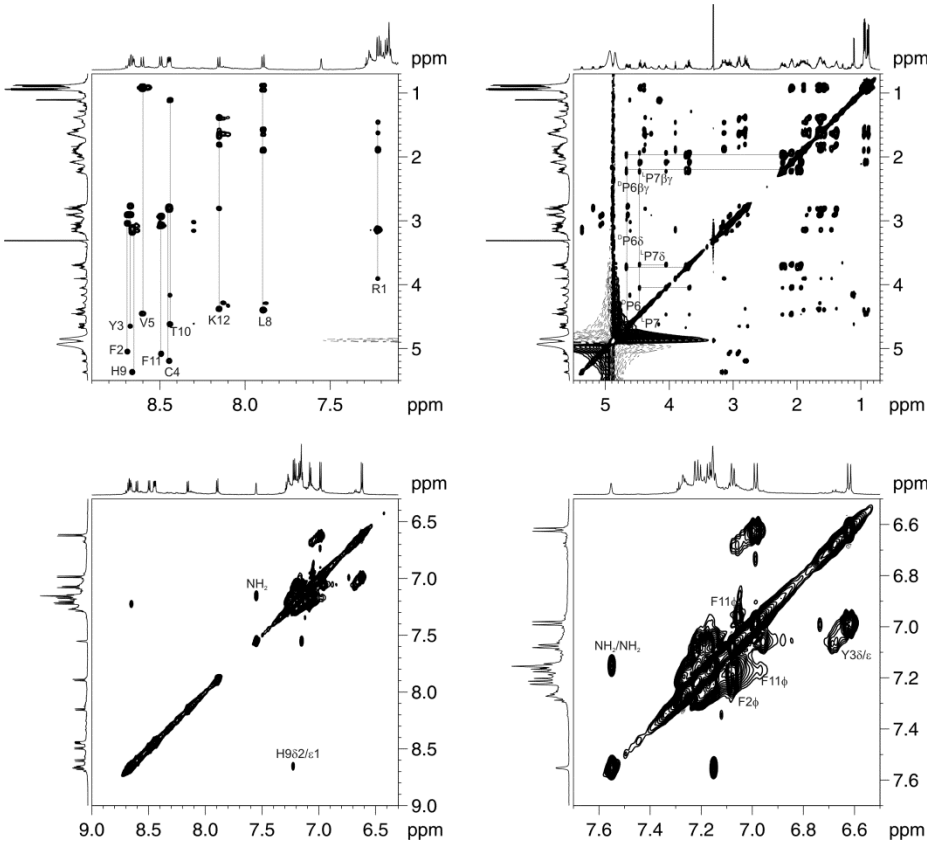

Res	NH	$C^{\alpha}H$	$C^{\beta}H$	Others	$^{3}J_{HN-C^{\alpha}H}$	dδ/dT
	ppm	ppm	ppm	ppm	Hz	ppb/K
R1	-	3.90	(1.88), (1.62)	$C^{\gamma}H$: (1.45) $C^{\delta}H$: 3.14	-	-
F2	8.69	5.04	3.04, 2.90	$C^{\phi}H$: 7.17	8.32	-7.5
Y3	8.67	4.65	2.90, 2.77	$C^{\delta}H$: 6.98 $C^{\varepsilon}H$: 6.62	8.82	-5.75
C4	8.45	5.19	2.80	-	9.01	-10.0
V5	8.60	4.45	2.08	$C^{\gamma}H$: 0.91	9.46	-4.25
^{D}P6	-	4.67	(2.24)	$C^{\gamma}H$: 1.98 $C^{\delta}H$: 3.73	-	-
^{L}P7	-	4.46	(2.22)	$C^{\gamma}H$:(1.93) $C^{\delta}H$: 4.05, 3.68	-	-
L8	7.89	4.40	1.89	$C^{\gamma}H$: 1.57 $C^{\delta}H$: 0.95, 0.87	8.26	-1.25
H9	8.66	5.36	(3.17), (3.12)	$C^{\delta 2}H$: 7.22 $C^{\varepsilon 1}H$: 8.67	8.44	-8.25
T10	8.43	4.62	4.16	$C^{\gamma}H$: 1.11	8.13	-5.75
F11	8.49	5.08	3.07, 2.93	$C^{\phi}H$: 7.08	8.13	-7.0
K12	8.15	4.38	(1.80)	$C^{\gamma}H$:1.38 $C^{\delta}H$: 1.67 $C^{\varepsilon}H$: 2.80	8.09	-5.0

Figure S5 (a): Partial expansion of the TOCSY spectrum (top) and chemical shift table (bottom) for **C4H9** recorded in CD_3OH at 298K.

Supplementary Material (ESI) for Physical Chemistry Chemical Physics
This journal is © The Royal Society of Chemistry 2013

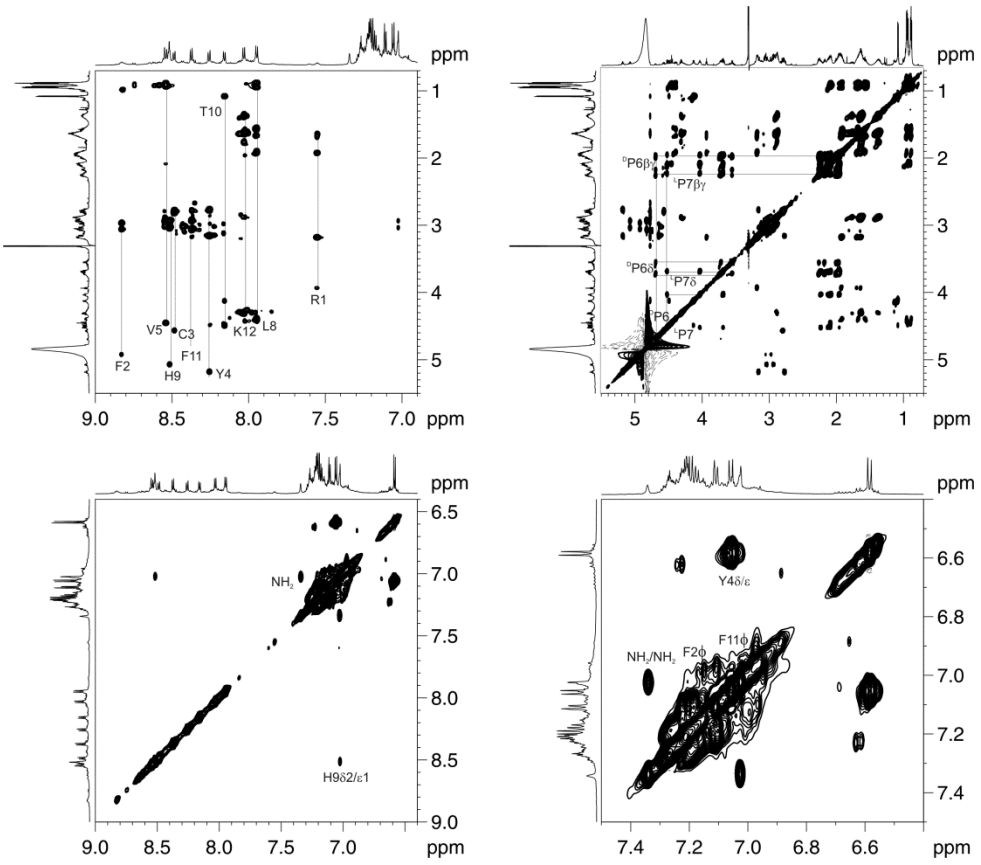

Res	NH	$C^{\alpha}H$	$C^{\beta}H$	Others	$^{3}J_{HN\text{-}C^{\alpha}H}$	dδ/dT
	ppm	ppm	ppm	ppm	Hz	ppb/K
R1	7.55	3.93	(1.92)	$C^{\gamma}H$: (1.64) $C^{\delta}H$: 3.18	6.91	-
F2	8.82	4.92	3.05, 2.96	$C^{\phi}H$: 7.20	7.79	-6.75
C3	8.48	4.56	2.79	-	8.20	-5.00
Y4	8.25	5.18	3.15, 2.76	$C^{\delta}H$: 7.05 $C^{\varepsilon}H$: 6.58	8.94	-8.5
V5	8.54	4.45		$C^{\gamma}H$: 0.90	9.24	-5.25
^{D}P6	-	4.69	(2.25), (2.17)	$C^{\gamma}H$: (1.98) $C^{\delta}H$: 3.72, 3.55	-	-
^{L}P7	-	4.51	(2.22), (2.11)	$C^{\gamma}H$: (1.95) $C^{\delta}H$: 4.03, 3.68	-	-
L8	7.94	4.39	(1.91)	$C^{\gamma}H$: (1.56) $C^{\delta}H$: (0.94), (0.87)	8.10	-1.75
H9	8.51	5.07	(3.03), (2.93)	$C^{\delta 2}H$: 7.02 $C^{\varepsilon 1}H$: 8.51	8.27	-8.75
T10	8.15	4.48	4.12	$C^{\gamma}H$: 1.08	8.02	-4.25
F11	8.37	4.82	(3.06), (2.92)	$C^{\phi}H$: 7.11	8.07	-7.0
K12	8.03	4.31	(1.76)	$C^{\gamma}H$:1.36 $C^{\delta}H$: 1.62 $C^{\varepsilon}H$: 2.88	8.20	-4.75

Figure S5 (b): Partial expansion of the TOCSY spectrum (top) and chemical shift table (bottom) for **Y4H9** recorded in CD_3OH at 308K.

Supplementary Material (ESI) for Physical Chemistry Chemical Physics
This journal is © The Royal Society of Chemistry 2013

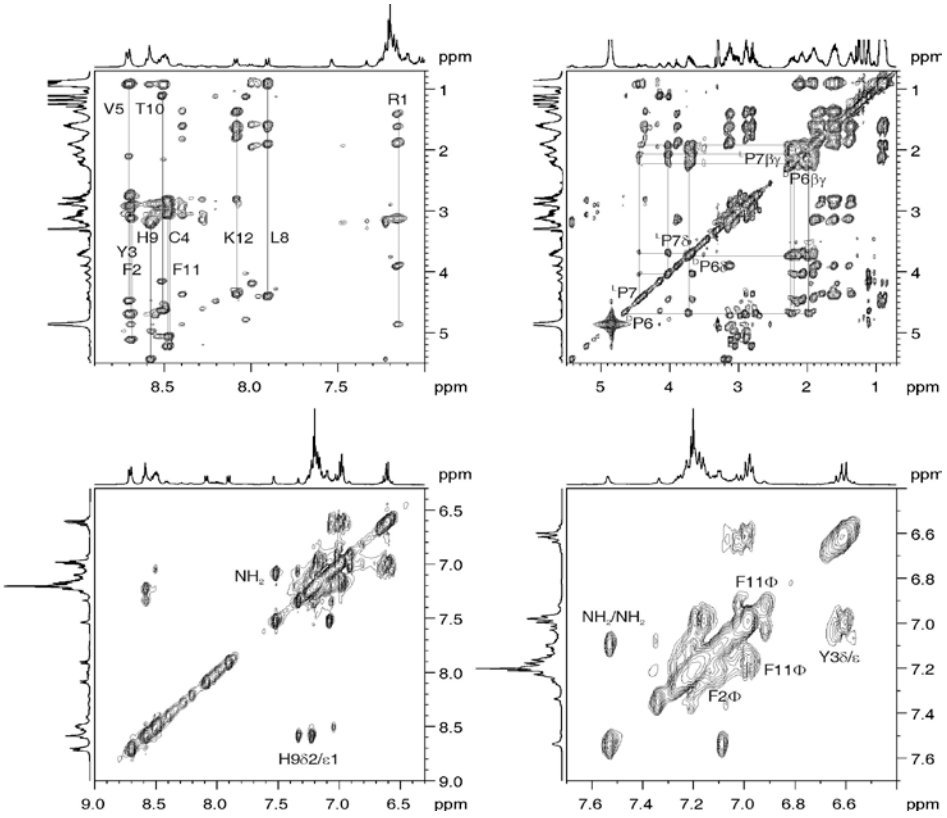

Res.	NH	$C^{\alpha}H$	$C^{\beta}H$	Others	$^{3}J_{HN\text{-}C^{\alpha}H}$	dδ/dT
	ppm	ppm	ppm	ppm	Hz	ppb/K
R1	-	3.91	(1.90), (1.59)	$C^{\gamma}H$: (1.35) $C^{\delta}H$: 3.14	-	-
F2	8.71	5.11	3.15	$C^{\phi}H$: 7.20	9.2	-6.0
Y3	8.71	4.70	2.88, 2.79	$C^{\delta}H$: 6.99 $C^{\varepsilon}H$: 6.61	9.2	-2.5
C4	8.50	5.22	3.05, 2.86	*t*Bu : 1.19	9.0	-12.8
V5	8.71	4.46	2.08	$C^{\gamma}H$: 0.94	9.2	-4.0
^{D}P6	-	4.67	(2.22)	$C^{\gamma}H$: (1.95) $C^{\delta}H$: 3.74	-	-
^{L}P7	-	4.43	(2.22), (2.08)	$C^{\gamma}H$: (1.91) $C^{\delta}H$: 3.68	-	-
L8	7.91	4.40	(1.90)	$C^{\gamma}H$: (1.61) $C^{\delta}H$: 0.87	8.2	-2.0
H9	8.59	5.43	3.19	$C^{\delta 2}H$: 7.23 $C^{\varepsilon 1}H$: 8.59	8.8	-10.5
T10	8.53	4.63	4.15	$C^{\gamma}H$: 1.11	8.4	-5.0
F11	8.48	5.04	3.00, 2.83	$C^{\phi}H$: 7.17, 6.97	8.0	-8.8
K12	8.09	4.36	(1.78)	$C^{\gamma}H$: (1.64) $C^{\delta}H$: (1.37) $C^{\varepsilon}H$: 2.84	8.1	-4.5

Figure S5 (c): Partial expansion of the TOCSY spectrum (top) and chemical shift table (bottom) for **C4H9-p** recorded in CD_3OH at 303K.

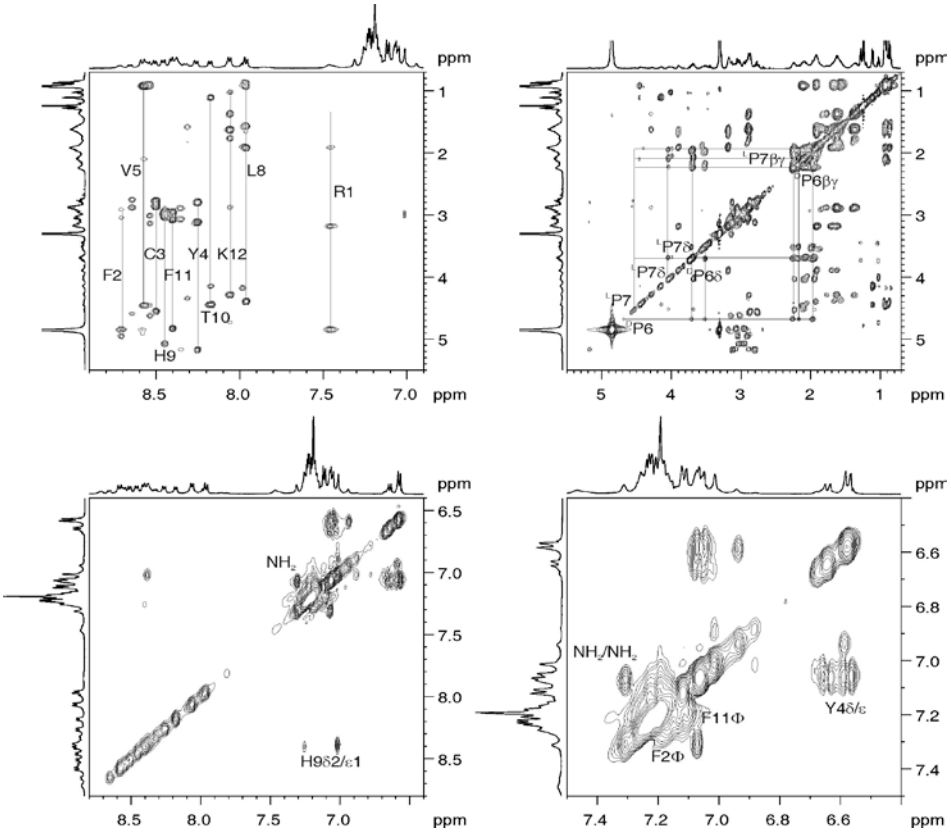

Res.	NH	$C^{\alpha}H$	$C^{\beta}H$	Others	$^{3}J_{HN\text{-}C^{\alpha}H}$	dδ/dT
	ppm	ppm	ppm	ppm	Hz	ppb/K
R1	-	3.89	(1.92)	$C^{\gamma}H$: (1.65) $C^{\delta}H$: 3.18	-	-
F2	8.73	4.95	3.06, 2.89	$C^{\Phi}H$: 7.23	~3.0	-9.3
C3	8.51	4.57	2.86, 2.77	*t*Bu : 1.24	8.2	-7.8
Y4	8.27	5.18	3.11, 2.82	$C^{\delta}H$: 7.05 $C^{\varepsilon}H$: 6.58	8.8	-11.5
V5	8.58	4.45	2.09	$C^{\gamma}H$: 0.93	9.4	-5.0
^{D}P6	-	4.69	(2.24), (2.12)	$C^{\gamma}H$: (1.89) $C^{\delta}H$: 3.72, 3.56	-	-
^{L}P7	-	4.54	(2.24), (2.12)	$C^{\gamma}H$: (1.92) $C^{\delta}H$: 3.68	-	-
L8	7.97	4.28	(1.96)	$C^{\gamma}H$: (1.55) $C^{\delta}H$: 0.88	9.1	-0.5
H9	8.46	5.07	3.03, 2.91	$C^{\delta 2}H$: 7.02 $C^{\varepsilon 1}H$: 8.39	8.3	-8.5
T10	8.19	4.43	4.15	$C^{\gamma}H$: 1.11	7.7	-5.8
F11	8.42	4.84	3.06, 2.88	$C^{\Phi}H$: 7.18, 7.12	7.6	-10.8
K12	8.07	4.29	(1.63)	$C^{\gamma}H$: (1.37) $C^{\delta}H$: (1.02) $C^{\varepsilon}H$: 2.85	7.6	-5.3

Figure S5 (d): Partial expansion of TOCSY spectrum (top) and chemical shift table (bottom) for **Y4H9-p** recorded in CD_3OH at 303K.

Supplementary Material (ESI) for Physical Chemistry Chemical Physics
This journal is © The Royal Society of Chemistry 2013

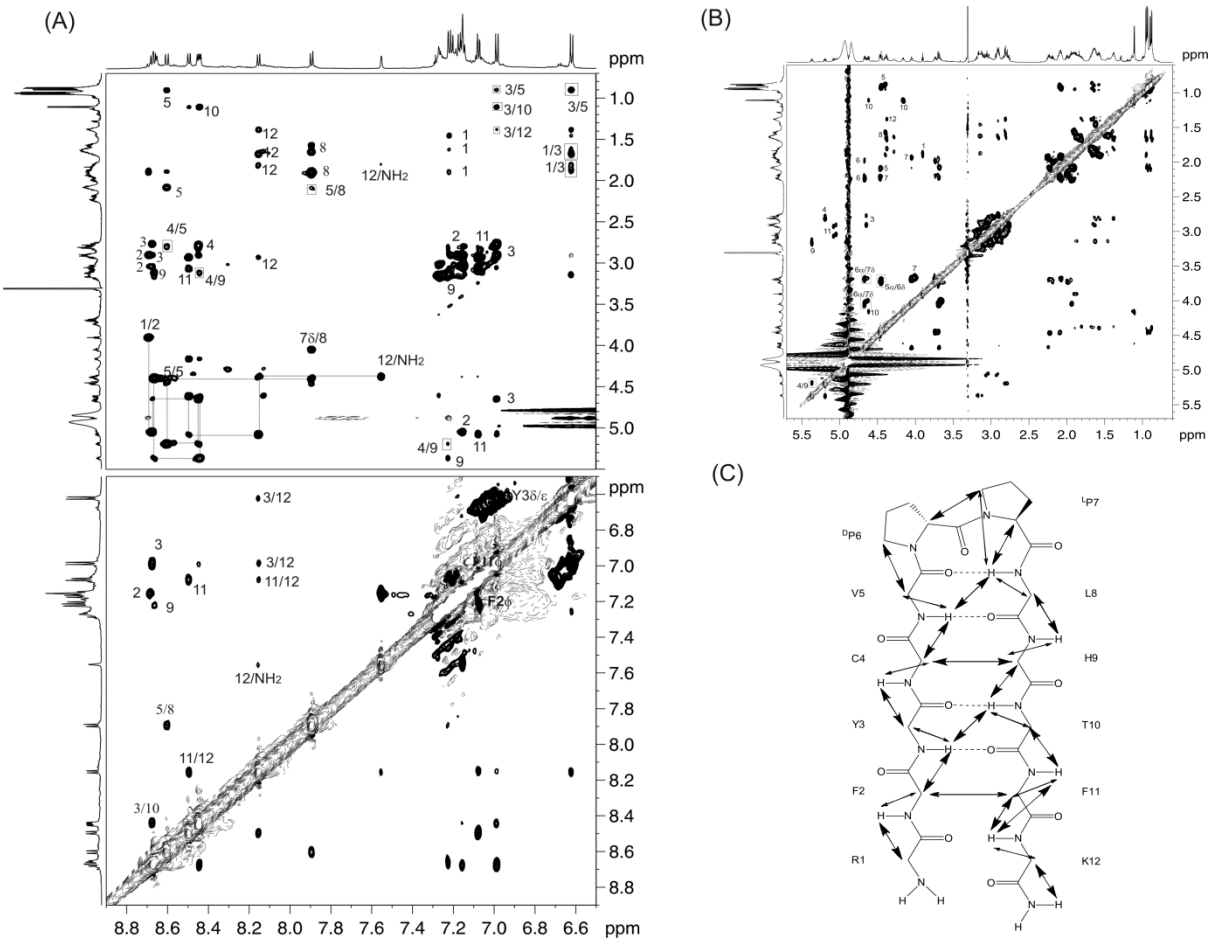

Figure S6 (a): Partial expansions of ROESY spectrum of **C4H9** in CD_3OH at 298K. (A) Expansions of NH-NH (bottom) and NH-$C^{\alpha/\beta}H$ (top) region of ROESY spectrum. (B) Expansion of $C^{\alpha/\beta}H$ region. Diagnostic hairpin NOEs and backbone connectivity are annotated. (C) Schematic representation of observed backbone NOEs marked as double-edged arrows. Observed hydrogen bonds are indicated as dashed lines.

Supplementary Material (ESI) for Physical Chemistry Chemical Physics
This journal is © The Royal Society of Chemistry 2013

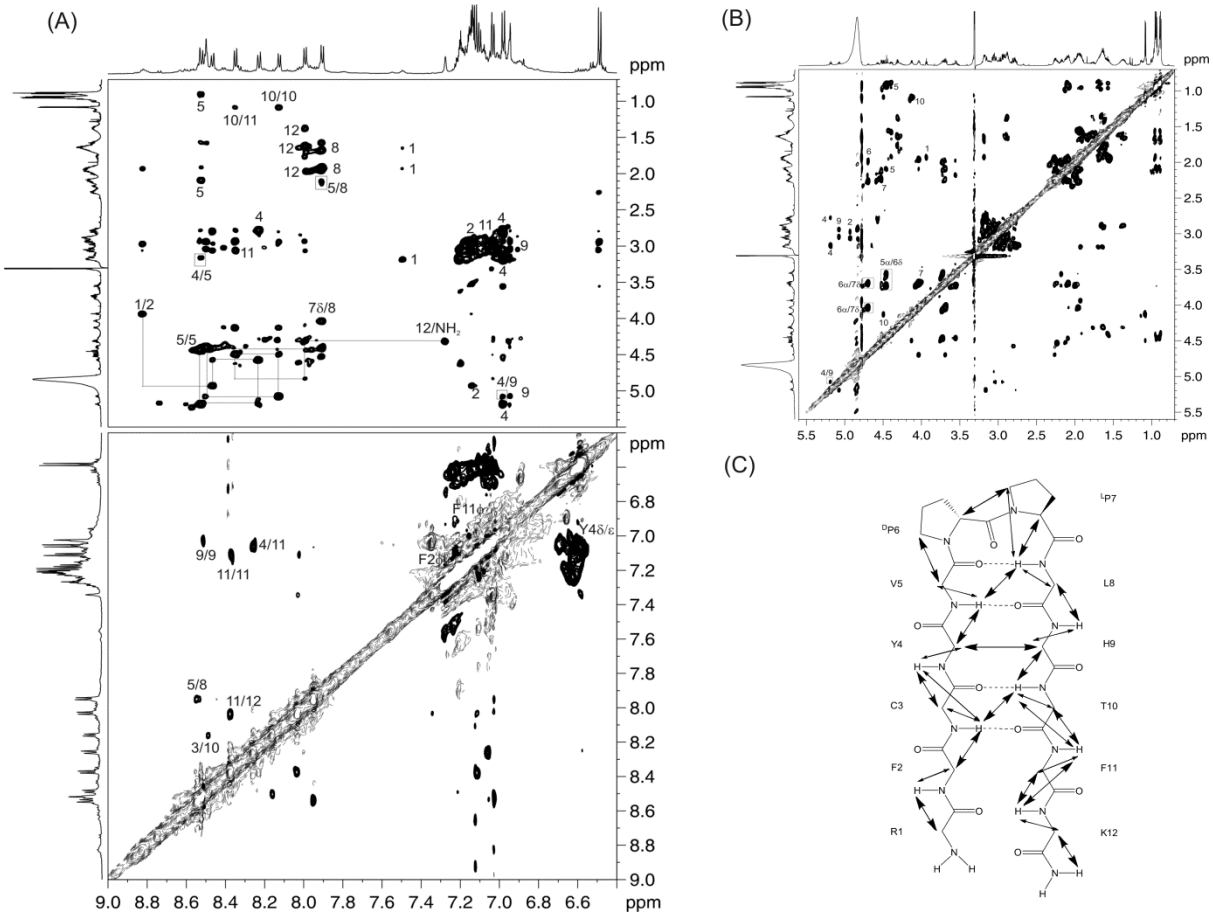

Figure S6 (b): Partial expansions of ROESY spectrum of **Y4H9** in CD_3OH at 308K. (A) Expansions of NH-NH (bottom) and NH-$C^{\alpha/\beta}H$ (top) region of ROESY spectrum. (B) Expansion of $C^{\alpha/\beta}H$ region. Diagnostic hairpin NOEs and backbone connectivity are annotated. (C) Schematic representation of observed backbone NOEs marked as double-edged arrows. Observed hydrogen bonds are indicated as dashed lines.

Supplementary Material (ESI) for Physical Chemistry Chemical Physics
This journal is © The Royal Society of Chemistry 2013

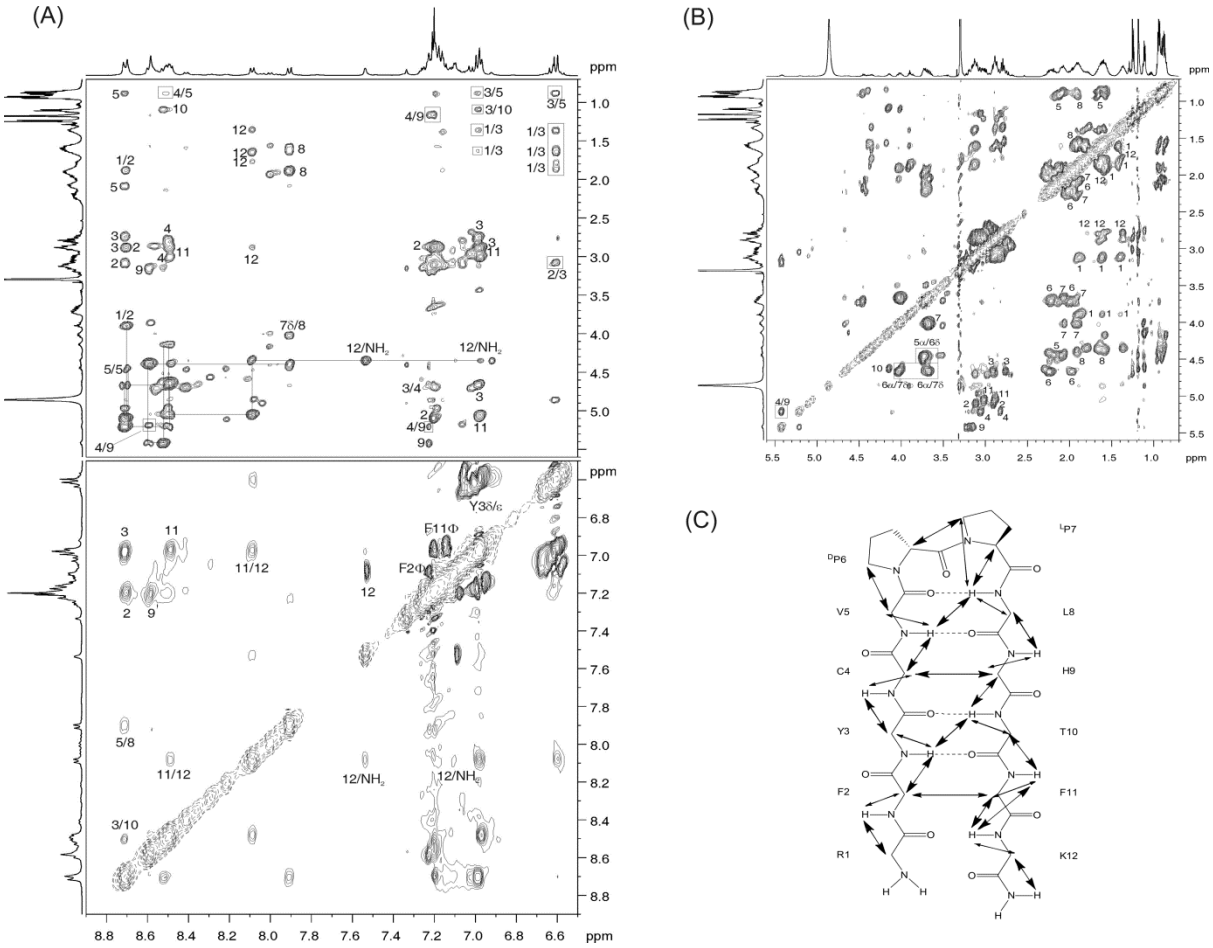

Figure S6 (c): Partial expansions of ROESY spectrum of **C4H9-p** in CD_3OH at 303K. (A) Expansions of NH-NH (bottom) and NH-$C^{\alpha/\beta}H$ (top) region of ROESY spectrum. (B) Expansion of $C^{\alpha/\beta}H$ region. Diagnostic hairpin NOEs and backbone connectivity are annotated. (C) Schematic representation of observed backbone NOEs marked as double-edged arrows. Observed hydrogen bonds are indicated as dashed lines.

Supplementary Material (ESI) for Physical Chemistry Chemical Physics
This journal is © The Royal Society of Chemistry 2013

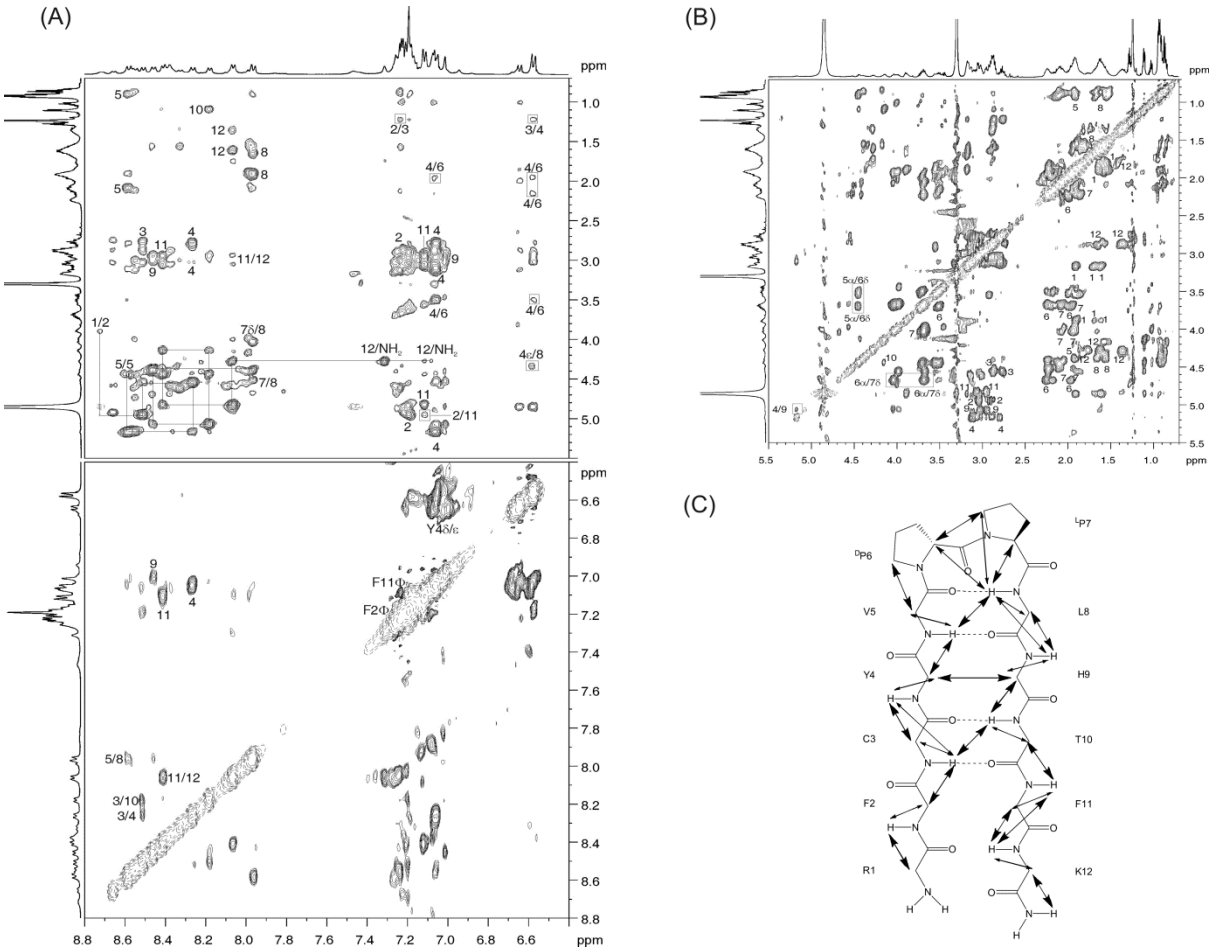

Figure S6 (d): Partial expansions of ROESY spectrum of **Y4H9-p** in CD_3OH at 303K. (A) Expansions of NH-NH (bottom) and NH-$C^{\alpha/\beta}H$ (top) region of ROESY spectrum. (B) Expansion of $C^{\alpha/\beta}H$ region. Diagnostic hairpin NOEs and backbone connectivity are annotated. (C) Schematic representation of observed backbone NOEs marked as double-edged arrows. Observed hydrogen bonds are indicated as dashed lines.

Supplementary Material (ESI) for Physical Chemistry Chemical Physics
This journal is © The Royal Society of Chemistry 2013

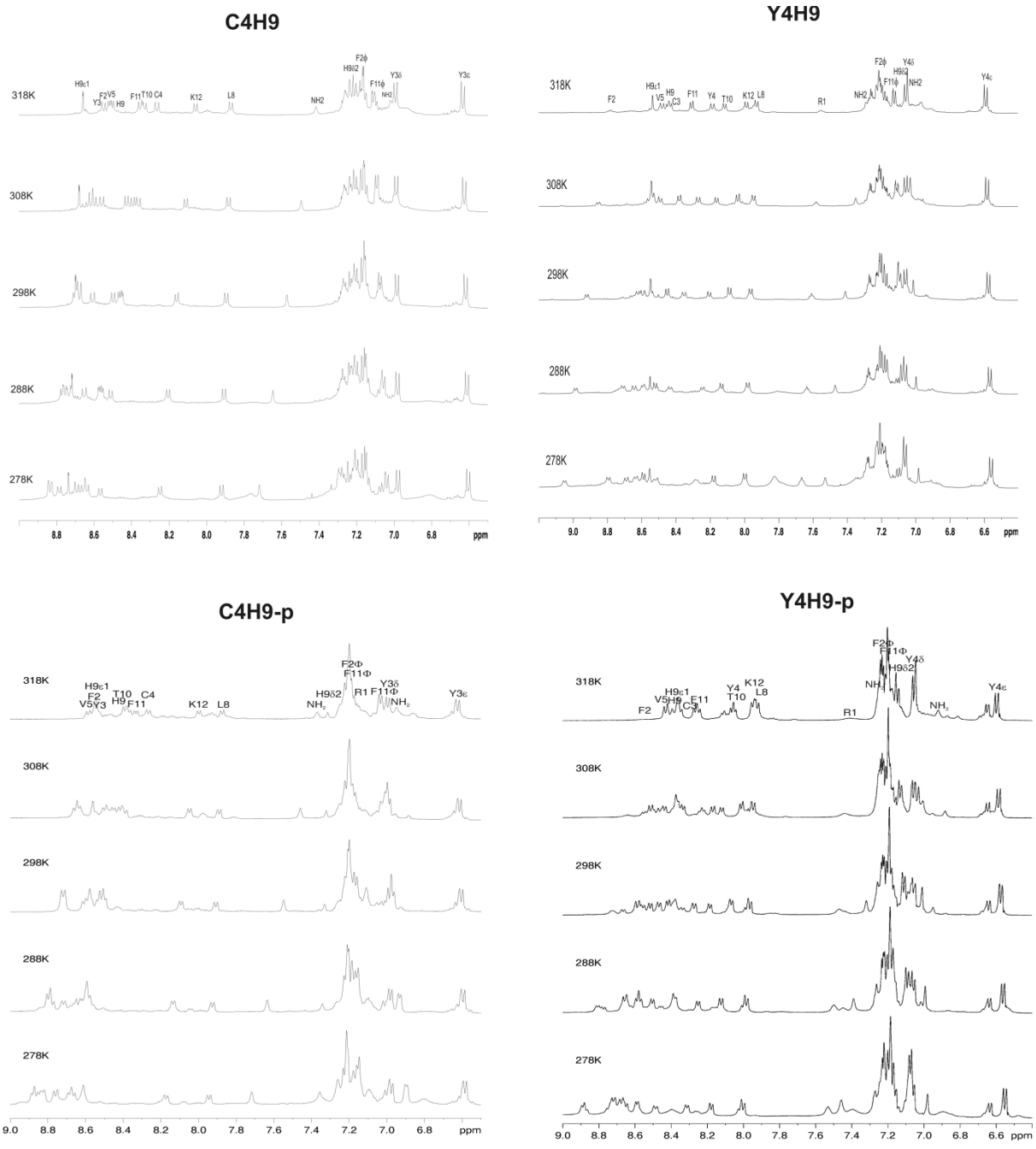

Figure S7: Change in the amide region of the ^{1}H 1D spectrum for all four peptides shown as a function of temperature. Solvent exposed amides show larger temperature dependent chemical change as compared to amides involved in intramolecular hydrogen bonding in all four peptides.

Supplementary Material (ESI) for Physical Chemistry Chemical Physics
This journal is © The Royal Society of Chemistry 2013

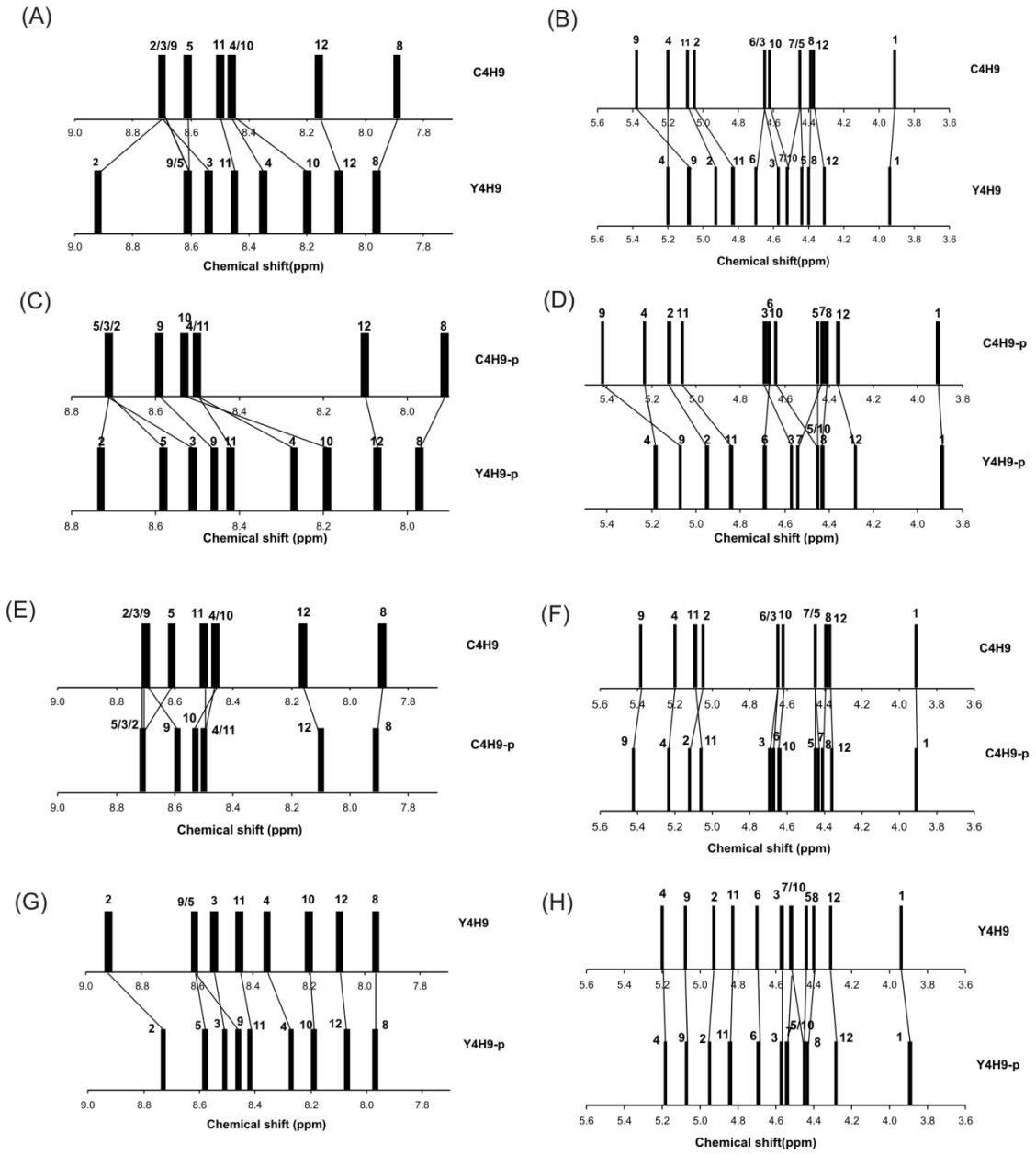

Figure S8: Stick plots comparing the backbone NH and $C^{\alpha}H$ shifts across the peptides in CD_3OH at 298K (**C4H9** and **Y4H9**) and 303K (**C4H9-p** and **Y4H9-p**). Here A, C, E and G show comparisons of the backbone NH chemical shifts and B, D, F and H compare $C^{\alpha}H$ chemical shifts. A-D show comparisons across the two peptides and their thiol protected analogues. E-H illustrate comparison of the effect of the thiol protection on the backbone chemical shifts in either peptide. It is noteworthy that substantial differences in backbone chemical shifts are observed between **C4H9** and **Y4H9** (A-D), indicating differences in their folded populations. On the contrary, thiol protection alone does not alter the secondary structure content, as is evident from the comparisons in E-H.

Supplementary Material (ESI) for Physical Chemistry Chemical Physics
This journal is © The Royal Society of Chemistry 2013

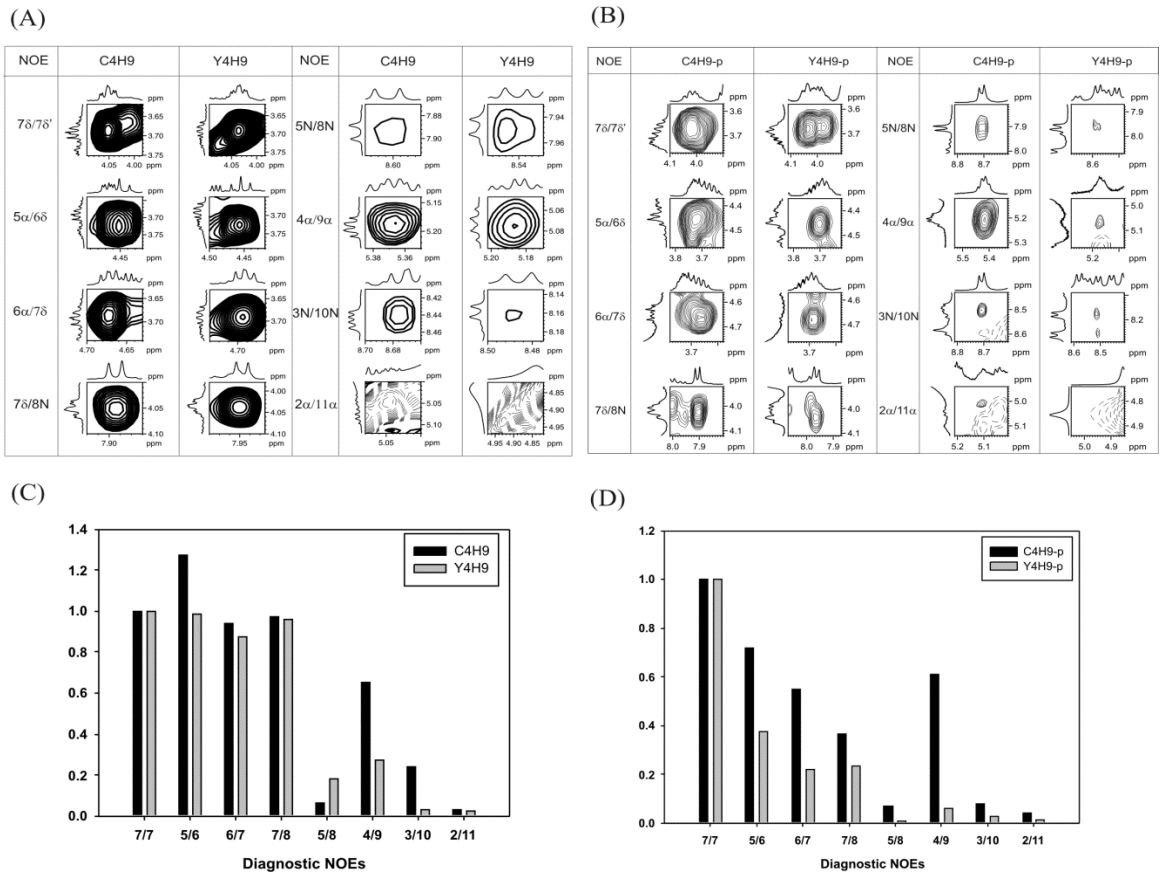

Figure S9: Comparison of diagnostic hairpin NOEs (A, B) and NOE intensity plots (C, D) (continued from Fig. 2 of the main text). (A, B) Diagnostic hairpin NOEs of **C4H9** and **Y4H9** (A) and **C4H9-p** and **Y4H9-p** (B). The cross peak between the geminal protons of δ and δ' of ^{L}Pro7 was used as a reference in each peptide, to compare other NOE intensities. Weak NOEs were uniformly scaled across peptides for purposes of display and comparison. The 5α/6δ and 6α/7δ NOEs confirm the *trans* conformation of Val5-^{D}Pro6 and ^{D}Pro6-^{L}Pro7 peptide units, respectively. These, along with 7δ/8N NOE, establish the existence of a type II' turn. The inter-strand 5N/8N and 3N/10N NOEs indicate the presence of the first and second pair of hydrogen bonds, respectively. The 4α/9α and 2α/11α NOEs are diagnostic of strand registry (although the 2α/11α NOE falls close to the water suppression, it must be noted that this NOE is weak in Cys-His pair but absent in Tyr-His pair, indicating poorer strand registry in the latter, towards the termini). The 1N-12N NOE was not observed, as the NH of Arg1 was in exchange with solvent. NOE intensity plots (C, D) were generated from densitometry analysis carried out using Multigauge v 2.3. The 7δ/δ', which was used as the reference, was normalized to 1.0. Other intensities were quantified with reference to this NOE. Overall intensities are stronger in the peptides with a Cys-His pair (**C4H9** and **C4H9-p**) as compared to the Tyr-His pair (**Y4H9** and **Y4H9-p**), indicating that a large population of the peptides with Cys-His pair adopt a folded hairpin conformation as compared to its Tyr-His counterpart. Additionally, protection of the

Cys side chain with *t*Bu does not substantially alter the folded population in both cases, suggesting that the presence of a free SH may not be required for this stabilizing Cys-His interaction.

Supplementary Material (ESI) for Physical Chemistry Chemical Physics
This journal is © The Royal Society of Chemistry 2013

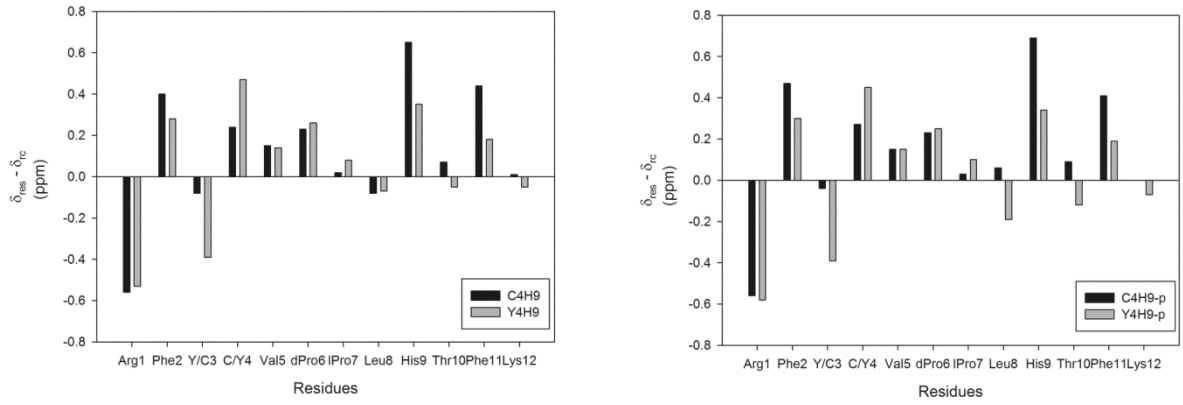

Figure S10: Chemical shift indexing (continued from Figure 1). Plot of H^{α} chemical shift deviation from the random coil values (δ_{res}–δ_{rc}) clearly indicates larger positive values for **C4H9**/**C4H9-p** as compared to **Y4H9**/**Y4H9-p**, especially towards the C-terminal segment.

Table S2: Calculated free energies of folding for the various peptides described in this study, obtained using NMR chemical shifts.

Peptide name	Sequence	Thermodynamic parameters[a]		
		Fraction folded (f_F) (Average)	K_{eq}	ΔG_F (kcal/mol)
C4H9	H_2N-RFYCV^{D}P^{L}PLHTFK-$CONH_2$	0.58	1.36	-0.18
Y4H9	H_2N-RFCYV^{D}P^{L}PLHTFK-$CONH_2$	0.28	0.39	+0.55
C4H9-p	H_2N-RFYC(*t*Bu)V^{D}P^{L}PLHTFK-$CONH_2$	0.61	1.54	-0.25
Y4H9-p	H_2N-RFC(*t*Bu)YV^{D}P^{L}PLHTFK-$CONH_2$	0.22	0.29	+0.75

[a]All calculations were carried out assuming T = 298K for the first two peptides and T = 303K for the thiol protected analogues. Arg1 was not included in the calculation, since the chemical shift was influenced by the amide resonance undergoing exchange in solution. Additionally Tyr 3/4 and Cys4/3 were also not included, since these resonances exhibited a positional effect of chemical shift, in addition to the contribution from the folded↔unfolded equilibrium of the peptide. Such observations have been made earlier,[8] and including such anomalous chemical shifts may lead to erroneous thermodynamic parameters. Chemical shifts of residues in the unfolded and folded conformations were obtained from the BMRB.[9]

Supplementary Material (ESI) for Physical Chemistry Chemical Physics
This journal is © The Royal Society of Chemistry 2013

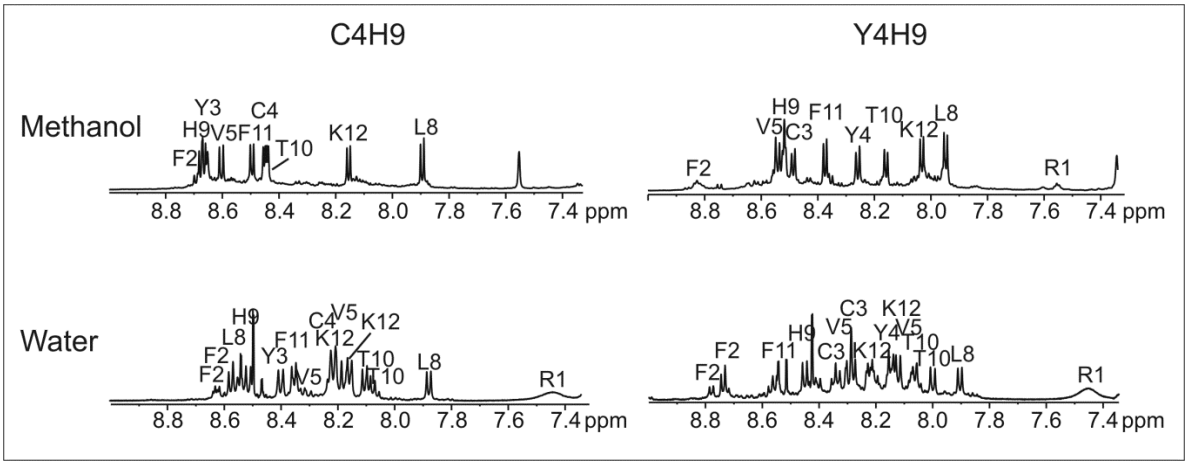

Figure S11: Comparison of ^{1}H 1D spectra of **C4H9** and **Y4H9** in methanol and water. Resonance assignments in water were achieved using TOCSY and ROESY experiments recorded at 303K (data not shown). Note the characteristic 'doubling' of resonances in water, indicating the existence of at least two peptide populations undergoing slow interconversion during NMR timescales. This arises primarily due to the *cis-trans* isomerization of the Xxx-$^{D/L}$Pro unit in aqueous solutions. Such conformational exchange is slow due to the large energy barrier involved in isomerization of the planar peptide unit. In the current peptides, such conformational interconversion leads to noticeable loss in secondary structure content, as deduced from CD experiments. Detailed analysis could not be carried out in water due to the lack of a significant folded peptide population in this solvent, coupled with spectral overlap due to the formation of multiple conformations.

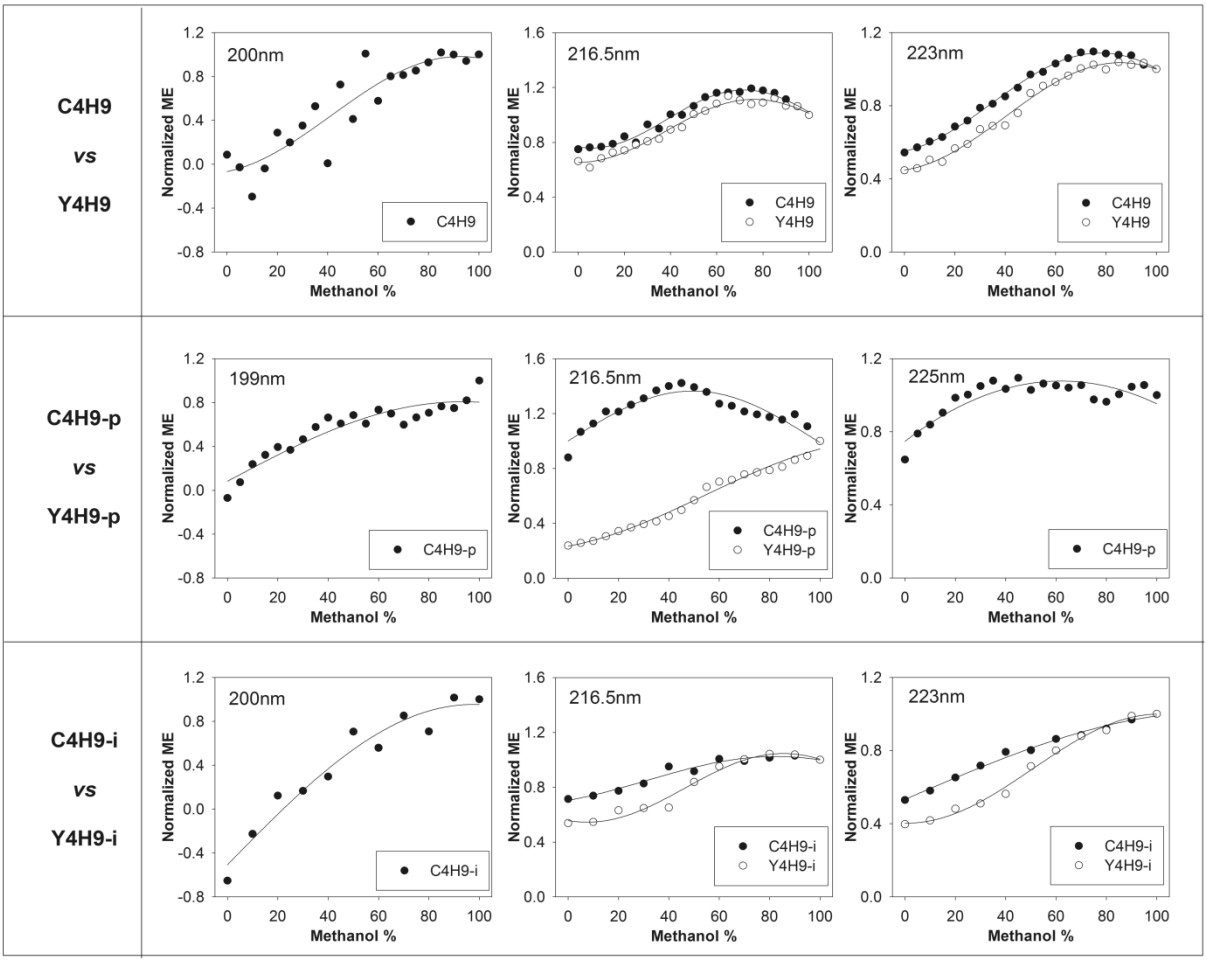

Figure S12: Comparison of the unfolding of **C4H9** *vs* **Y4H9** and its thiol protected analogues (**C4H9-p** and **Y4H9-p**: *t*Bu protected; **C4H9-i** and **Y4H9-i**: carbamidomethyl group protected, generated by treatment with iodoacetamide). The *y*-axis in each graph represents the molar ellipticity normalized to 1.0 in 100% methanol. This value also reflects the fraction folded in each peptide in aqueous methanol, and it was assumed that each peptide was 100% folded in methanol. Note that the titration indicates that ~75% methanol promotes more structure formation in both **C4H9** and **Y4H9**; ~50% aqueous methanol exhibits highest secondary structure content in the case of **C4H9-p**. Such increase in secondary structure content of peptides in aqueous methanol has been reported earlier.[8b, 13] **Y4H9** and its analogues showed no variation in some wavelengths and these plots are therefore not included in some cases. All spectra were recorded at 298K.

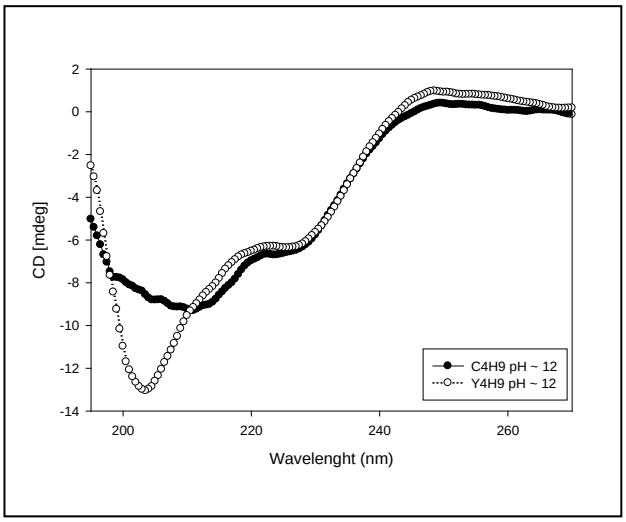

Figure S13: CD profile of **C4H9** and **Y4H9** in alkaline pH. To test the effect of pH as a destabilizing agent of peptide conformation, both peptides were dissolved in water and the pH was adjusted to ~12.0 using NaOH. Note the loss in CD signal below ~210nm. Based on previous reports,[13] this change in CD profile could correspond to an equilibrium between the β-hairpin structure and a random coil, in both peptides. The population of random coil is greater in **Y4H9**. Additionally, the negative maximum at ~215nm is more pronounced in **C4H9**, indicating that this sequence preferentially adopts an extended structure even in highly alkaline conditions, compared to **Y4H9**. As described earlier, CD spectra of short sequences are often complicated by contributions from aromatic residues, and must therefore be interpreted with caution.

Table S3: Summary of experimental constraints used for structure calculation for all four peptides and the observed violations.

Experimental constraint	# of constraints
C4H9	
Intraresidue NOEs	79
Sequential NOEs	18
Long range NOEs	12
Hydrogen bond constraints	4
Angle constraints	9
Y4H9	
Intraresidue NOEs	79
Sequential NOEs	19
Long range NOEs	4
Hydrogen bond constraints	4
Angle constraints	9
C4H9-p	
Intraresidue NOEs	79
Sequential NOEs	16
Long range NOEs	12
Hydrogen bond constraints	4
Angle constraints	9
Y4H9-p	
Intraresidue NOEs	79
Sequential NOEs	17
Long range NOEs	8
Hydrogen bond constraints	4
Angle constraints	9

Constraints violated in 33 or more structures (all four peptides):

VdW HA DPRO 6 - CD PRO 7

0 violated distance constraints.

1 violated van der Waals constraint.

0 violated angle constraints.

Table S4: Summary of backbone dihedral angles for 15 best structures of **C4H9**.

Residue	Phi[a]	Psi[a]
Arg 1	-	131.9 +/- 38.3
Phe 2	-137.5 +/- 61.1	141.3 +/- 21.1
Tyr 3	-136.3 +/- 24.4	123.7 +/- 42.7
Cys 4	-102.4 +/- 46.2	114.6 +/- 25.8
Val 5	-134.2 +/- 12.4	76.4 +/- 4.4
^{D}Pro 6	69.7 +/- 0.03	-123.8 +/- 10.7
^{L}Pro 7	-69.7 +/- 0.04	-11.8 +/- 14.1
Leu 8	-118.4 +/- 26.3	136.4 +/- 28.2
His 9	-123.2 +/- 31.0	147.6 +/- 27.3
Thr 10	-143.7 +/- 13.1	169.1 +/- 9.5
Phe 11	-129.3 +/- 13.7	56.5 +/- 5.1
Lys 12	-104.2 +/- 32.6	-

[a]Angles are in units of degrees.

Table S5: Summary of backbone dihedral angles for 15 best structures of **Y4H9**.

Residue	Phi[a]	Psi[a]
Arg 1	-	112.3 +/- 33.7
Phe 2	-89.2 +/- 78.2	114.4 +/- 30.6
Cys 3	-154.0 +/- 25.0	118.7 +/- 35.5
Tyr 4	-112.0 +/- 29.6	126.2 +/- 12.1
Val 5	-144.6 +/- 14.7	80.3 +/- 19.1
^{D}Pro 6	69.7 +/- 0.04	-119.0 +/- 14.2
^{L}Pro 7	-69.7 +/- 0.04	-18.7 +/- 13.1
Leu 8	-91.9 +/- 19.9	126.4 +/- 27.0
His 9	-141.6 +/- 45.9	128.5 +/- 35.3
Thr 10	22.4 +/- 93.6	164.8 +/- 10.2
Phe 11	-169.6 +/- 73.2	64.3 +/- 6.3
Lys 12	-65.5 +/- 63.8	-

[a]Angles are in units of degrees.

Table S6: Summary of backbone dihedral angles for 15 best structures of **C4H9-p**.

Residue	Phi[a]	Psi[a]
Arg 1	-	118.6 +/- 30.8
Phe 2	-100.0 +/- 95.3	128.2 +/- 22.8
Tyr 3	-148.7 +/- 27.3	124.9 +/- 43.1
Cys (S-*t*Bu) 4	-92.0 +/- 55.2	117.0 +/- 24.1
Val 5	-128.3 +/- 15.6	92.6 +/- 25.7
^{D}Pro 6	69.7 +/- 0.04	-119.9 +/- 12.5
^{L}Pro 7	-69.7 +/- 0.03	-16.3 +/- 22.9
Leu 8	-146.3 +/- 50.1	159.8 +/- 22.6
His 9	-137.9 +/- 23.5	174.2 +/- 63.9
Thr 10	-132.5 +/- 29.9	174.7 +/- 18.4
Phe 11	-142.7 +/- 22.2	60.4 +/- 9.1
Lys 12	-94.6 +/- 55.0	-

[a]Angles are in units of degrees.

Table S7: Summary of backbone dihedral angles for 15 best structures of **Y4H9-p**.

Residue	Phi[a]	Psi[a]
Arg 1	-	115.9 +/- 34.8
Phe 2	-131.8 +/- 107.2	121.4 +/- 23.8
Cys (S-*t*Bu) 3	-156.0 +/- 21.6	91.1 +/- 34.1
Tyr 4	-82.1 +/- 28.6	138.3 +/- 21.9
Val 5	-140.2 +/-13.4	82.5 +/- 17.6
^{D}Pro 6	69.7 +/-0.03	-123.1 +/- 8.86
^{L}Pro 7	-69.7 +/- 0.03	-20.1 +/- 16.4
Leu 8	-108.1 +/- 26.0	157.9 +/- 20.8
His 9	-129.8 +/- 18.6	155.0 +/- 20.5
Thr 10	-76.9 +/- 61.5	159.2 +/- 10.9
Phe 11	-172.7 +/- 80.4	64.2 +/- 6.3
Lys 12	-55.9 +/- 82.4	-

[a]Angles are in units of degrees.

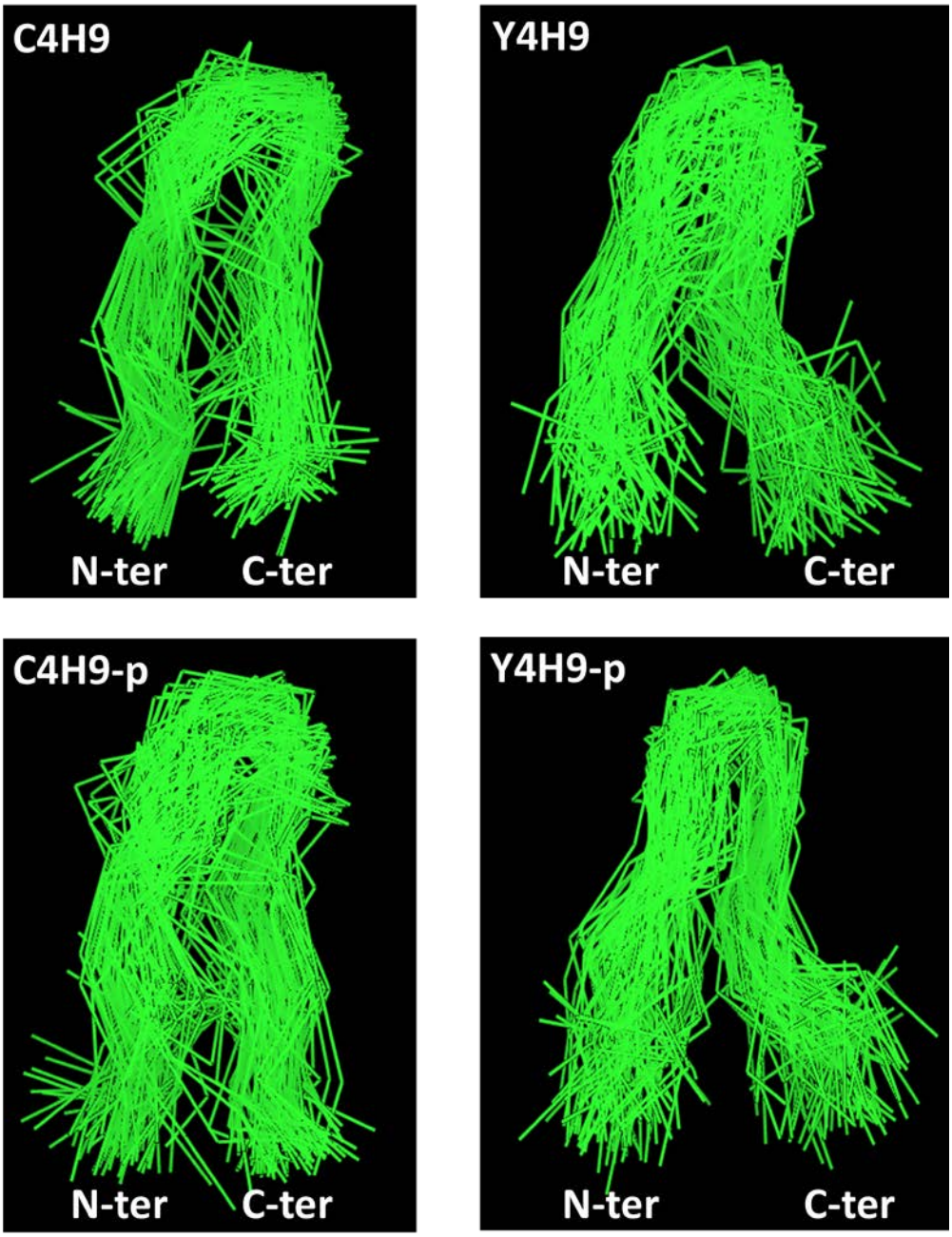

Figure S14: Superposition of 100 calculated structures for each peptide using CYANA v2.1. N- and C-termini are indicated as N-ter and C-ter, respectively. Note the greater strand fraying towards the termini in the case of **Y4H9** and **Y4H9-p**. Average backbone RMSDs for all 100 structures, derived from CYANA, are as follows: **C4H9** = 1.39±0.61Å; **C4H9-p** = 1.59±0.68Å; **Y4H9** = 1.89±0.40 Å; **Y4H9-p** = 1.85±0.44Å. Average heavy atom RMSDs for all 100 structures are as follows: **C4H9** = 2.58±0.91Å; **C4H9-p** = 2.90±1.03Å; **Y4H9** = 3.31±0.50 Å; **Y4H9-p** = 3.22±0.56Å.

References

1. R. Rai, S. Raghothama and P. Balaram, *J. Am. Chem. Soc.*, 2006, **128**, 2675-2681.
2. (a) C. Grathwohl and K. Wuthrich, *Biopolymers*, 1976, **15**, 2025-2041; (b) G. N. Ramachandran and A. K. Mitra, *J. Mol. Biol.*, 1976, **107**, 85-92; (c) M. W. MacArthur and J. M. Thornton, *J. Mol. Biol.*, 1991, **218**, 397-412; (d) U. Reimer, G. Scherer, M. Drewello, S. Kruber, M. Schutkowski and G. Fischer, *J. Mol. Biol.*, 1998, **279**, 449-460; (e) D. Pal and P. Chakrabarti, *J. Mol. Biol.*, 1999, **294**, 271-288; (f) R. Bhattacharyya and P. Chakrabarti, *J. Mol. Biol.*, 2003, **331**, 925-940; (g) D. Pahlke, C. Freund, D. Leitner and D. Labudde, *BMC Struct. Biol.*, 2005, **5**, 8.
3. (a) S. K. Awasthi, S. Raghothama and P. Balaram, *Biochem. Biophys. Res. Commun.*, 1995, **216**, 375-381; (b) I. L. Karle, C. Das and P. Balaram, *Proc. Natl. Acad. Sci. U. S. A.*, 2000, **97**, 3034-3037; (c) C. Das, G. A. Naganagowda, I. L. Karle and P. Balaram, *Biopolymers*, 2001, **58**, 335-346; (d) C. Das, S. C. Shankaramma and P. Balaram, *Chemistry*, 2001, **7**, 840-847; (e) S. Aravinda, V. V. Harini, N. Shamala, C. Das and P. Balaram, *Biochemistry*, 2004, **43**, 1832-1846; (f) V. V. Harini, S. Aravinda, R. Rai, N. Shamala and P. Balaram, *Chemistry*, 2005, **11**, 3609-3620.
4. (a) M. B. Swindells, M. W. MacArthur and J. M. Thornton, *Nat. Struct. Biol.*, 1995, **2**, 596-603; (b) S. R. Griffiths-Jones, G. J. Sharman, A. J. Maynard and M. S. Searle, *J. Mol. Biol.*, 1998, **284**, 1597-1609; (c) P. Koehl and M. Levitt, *Proc. Natl. Acad. Sci. U. S. A.*, 1999, **96**, 12524-12529.
5. M. Ramirez-Alvarado, F. J. Blanco and L. Serrano, *Nat. Struct. Biol.*, 1996, **3**, 604-612.
6. (a) S. Aravinda, N. Shamala, R. Rajkishore, H. N. Gopi and P. Balaram, *Angew. Chem. Int. Ed. Engl.*, 2002, **41**, 3863-3865; (b) R. Meurisse, R. Brasseur and A. Thomas, *Biochim. Biophys. Acta*, 2003, **1649**, 85-96; (c) R. Mahalakshmi, S. Raghothama and P. Balaram, *J. Am. Chem. Soc.*, 2006, **128**, 1125-1138; (d) A. Rajagopal, S. Aravinda, S. Raghothama, N. Shamala and P. Balaram, *Biopolymers*, 2012, **98**, 185-194.
7. H. E. Gottlieb, V. Kotlyar and A. Nudelman, *J. Org. Chem.*, 1997, **62**, 7512-7515.
8. (a) M. S. Searle, *J. Chem. Soc., Perkin Trans. 2*, 2001, 1011-1020; (b) M. Dhanasekaran, O. Prakash, Y. X. Gong and P. W. Baures, *Org Biomol Chem*, 2004, **2**, 2071-2082.
9. E. L. Ulrich, H. Akutsu, J. F. Doreleijers, Y. Harano, Y. E. Ioannidis, J. Lin, M. Livny, S. Mading, D. Maziuk, Z. Miller, E. Nakatani, C. F. Schulte, D. E. Tolmie, R. Kent Wenger, H. Yao and J. L. Markley, *Nucleic Acids Res.*, 2008, **36**, D402-408.
10. (a) P. Guntert, C. Mumenthaler and K. Wuthrich, *J. Mol. Biol.*, 1997, **273**, 283-298; (b) P. Guntert, *Methods Mol. Biol.*, 2004, **278**, 353-378.
11. *The PyMOL Molecular Graphics System, Version 1.2r3pre, Schrödinger, LLC.*
12. R. Koradi, M. Billeter and K. Wuthrich, *J. Mol. Graph.*, 1996, **14**, 51-55, 29-32.
13. A. J. Maynard, G. J. Sharman and M. S. Searle, *J. Am. Chem. Soc.*, 1998, **120**, 1996-2007.